



# 2010 JOURNAL OF UNDERGRADUATE RESEARCH

# TABLE OF CONTENTS

4 LETTER FROM THE PRESIDENT

5 EDITORIAL STATEMENT  
EDITORIAL BOARD

## ARTS & HUMANITIES

7 “La abstracción en El Sur de Jorge Luis Borges”  
*Nikole Czapp*

13 “I Want My Future to Be Different”  
*Jessica Gruber*

20 Análisis del poema “Explico Algunas Cosas”  
*Heather Peters*

25 “Una Mirada a la vida de Miquel de Cervantes a través de la caracterización:  
A Glimpse into the Life of Miguel de Cervantes Through Characterization”  
*Kelly Smith*

## LIFE & SOCIAL SCIENCES

32 DNA Barcoding of Crayfish Species  
*Zach Berman, Emily K. Bongiorno*

47 An Analysis of the Effect of Pathogen-Associated Molecular Patterns (PAMPS) on  
Phagocytosis by Hyaline Amoebocyte Populations in the Earthworm *Eisenia hortensis*.  
*Laura L. Goodfield and Sheryl L. Fuller-Espie*

66 Effects of Recombinant Human Cytokines Gamma Interferon, IL-10, and IL-12  
on the Natural Killer-Like Response in *Eisenia hortensis* and its Method of Cytotoxicity  
*Katrina M. Hill and Sheryl L. Fuller-Espie*

- 84 Computational Studies of Novel Nano Substructures  
*Erin McCole and Brittany McIntyre*
- 99 Modeling Tetra Coordinate Cu(I) Binding Proteins  
*Robert E. De Vasto, Jeffery D. Evanseck, and Melinda A. Harrison*

#### **VISUAL ART INSERT**

Dina DiTaranto, "*The Bean Box*"

Mark Zirpoli, "*Shutterspeed Newsletter*"

Dina DiTaranto, "*Girl With Key*"

Dina DiTaranto, "*Triptych*"

Krista Macknovitz, "*Runners World Magazine*"

Kelly Mullen, "*Offshore Surf Magazine*"

Marcia McConnell, "*Hitched Wedding Magazine*"

Megan Brown, "*Younique Magazine*"

Meredith Rowe, "*Sycamore Identity Manual*"

Stephanie Saveoz, "*Element Identity Manual*"

# LETTER FROM THE PRESIDENT

To the Readers of Cabrini College's second Journal of Undergraduate Research:

It is an honor to author a letter of introduction for the second annual edition of the *Journal of Undergraduate Research*. To the Journal, its editorial board, and its contributors I offer my heartfelt appreciation for extending me the opportunity to address its readers.

When a private college can produce a text such as the *Journal of Undergraduate Research*, it signifies extraordinary commitment. The depth of talent, vision and dedication that an annual journal requires is an indicator of the quality of faculty and student relationships that flourish at Cabrini. The mentoring relationship between a faculty member and a student is a value-added enrichment, one tangible advantage among the many that will develop through an undergraduate research experience. Studies indicate that institutions demonstrate greater gains in learning, personal initiative and communication skill in their students because of the opportunities undergraduate research offers. With the literary venture of the Journal, student contributors and their faculty mentors work together and add vastly to the quality of their and their peers' educational experience.

Successful undergraduate research integrates each of the College's core values. Understandably, one needs vision to conceive of and follow through on a project to ascertain measurable outcomes. Surely, one must be dedicated to excellence to complete a project through the scientific method, evaluating results and reassessing one's goals. Undoubtedly, a student must respect a faculty mentor to resolve issues unearthed through experimentation and accept suggestions that will broaden a research project's scope. Finally, and perhaps most importantly, a student will draw on a strong sense of community to share research outcomes with student peers and faculty in the pages of this volume.

At the heart of undergraduate research is a rare transformational opportunity to learn, not just for the involved student, but also for faculty and peers, for the College community and for those whose lives may ultimately benefit through the experimentation, results and reporting of the selected research project.

Please join me in applauding the Journal's editorial staff and contributors to this publication, and in wishing each of them continued success in their future academic endeavors.

Sincerely,

Marie Angelella George, Ph.D.  
President

# EDITORIAL STATEMENT

The Cabrini College *Journal of Undergraduate Research* is dedicated to the discovery, promotion, and publication of outstanding work done annually by Cabrini undergraduates. The Journal's Editorial Board selects and cultivates the best work for inclusion. Drawn from the *Undergraduate Arts, Research, & Scholarship Symposium*— an annual event where students present and display their research to the College community— the Board seeks academically rigorous and distinctive efforts that demonstrate Cabrini students' evolution into public intellectuals with a firm grasp of the stakes and conventions of meaningful scholarship. Articles are selected for publication based on their scholarly and rhetorical quality. They are from all disciplines, and exemplify one or more of the following accomplishments:

- an original research project
- unique contribution to the scholarship of the students field
- a new interpretation of an intellectually important problem, phenomenon, or text
- an interdisciplinary endeavor that suggests innovative approach to an altogether new subject for scholarly inquiry.

The Board also considers for publication any work of artistic merit that demonstrates academic seriousness and intellectual ambition.

## CO-EDITORS

*John Cordes, Ph.D.*

Department of Communication

*David Dunbar, Ph.D.*

Department of Biology

*Darryl Mace, Ph.D.*

Department of History and  
Political Science

*Lisa Ratmansky*

Director, Center for Teaching and Learning

*Thomas Stretton, Ed.D.*

Department of Education

## EDITORIAL BOARD

*Jan Buzydlowski, Ph.D.*

Department of Information Science  
and Technology

*Sherry Fuller-Espie, Ph.D.*

Department of Biology

*Richie Gebauer*

Coordinator, Co-Curricular Programming

*Melinda Harrison, Ph.D.*

Department of Chemistry

*Jeanne Komp*

Department of Graphic Design

*Allison Mary Superneau*

Department of Biology (student)

*Melissa Terlecki, Ph.D.*

Department of Psychology

*Paul Wright, Ph.D.*

Department of English

ARTS & HUMANITIES

**“La abstracción en *El Sur* de Jorge Luis Borges”**

Nikole Czapp

Faculty Advisor: Dr. Raquel Green

*The paper “La abstracción en El Sur de Jorge Luis Borges” was written by Nikole Czapp, a Spanish major in the Romance Languages and Literatures Department at Cabrini College, as part of the requirements for the Survey of Latin American Literature I course in the fall 2008. The literary analysis explores the Argentine author’s obsession with time in a complex, multilayered story which poses the question of whether dying by the knife in a duel is not a more dignified death for an Argentine than dying of septicemia in a hospital. Miss Czapp presented her paper in Spanish at the Honors Symposium in March 2009 at Neuman College in Aston, Pennsylvania and in April 2009 at Cabrini College’s Undergraduate Research Symposium.*

Jorge Luis Borges nos presenta con una visión escéptica del mundo en su cuento *El Sur*. *El Sur* es un relato que nos sumerge en la fabricación y la exageración. El protagonista de esta historia, Johannes Dahlmann, lleva a los lectores en un viaje donde la realidad y la ilusión se entrelazan y la verdadera existencia se cuestiona. Los acontecimientos que se producen en este breve resumen de la vida de Dahlmann son confusos en cuanto a si son reales o no. Borges quiere este escepticismo en su cuento para alentar a los lectores a crear su propia interpretación de lo que tiene lugar dentro del tiempo. Haciendo un juego con el tiempo, Borges propone modos diferentes de interpretar el cuento. No hay una fijación del tiempo en el cuento y, por esta razón, los lectores se ven ante una realidad confusa.

Juan Dahlmann es un argentino de ascendencia alemana cuyo trabajo diario es el de secretario de una biblioteca. Un día él recoge el libro, *Mil y una noches* y lo lleva a



su casa muy ansioso por leerlo. Al subir las escaleras corriendo, Dahlmann se golpea su cabeza en la arista de un batiente recién pintado. El accidente resulta en un corte en la cabeza y las complicaciones lo fuerzan a permanecer en cama con fiebre muy alta durante unos pocos días. A este punto, el personaje pierde control de la realidad. Durante esta etapa, “las ilustraciones de las *Mil y una noches* sirvieron para decorar pesadillas” (Borges 194).

Por ocho días Dahlmann guarda cama, pero a él le parece como si fueran ocho siglos. El estado febril del personaje sirve para hacer una superimposición del tiempo de tal manera que se pierde toda noción exacta del mismo. No hay restricciones del tiempo y Borges cuestiona la experiencia humana del tiempo. Borges piensa que en un instante pueden pasar siglos, todo depende de lo que ese instante represente en la vida de un ser humano. Borges busca darnos aquí evidencia que Dahlmann tiene un sentido de la realidad diferente al resto de la sociedad.

Eventualmente su enfermedad progresa y él debe trasladarse al sanatorio. Cuando está en el hospital a Dahlmann le parece como si estuviera en un infierno porque el dolor era muy fuerte. El estaba muy cerca de la muerte por septicemia y el pensamiento de la muerte termina obsesionándolo. La asociación del hospital con el infierno es desafortunado para él porque hace que él “...odió su identidad, sus necesidades corporales, su humillación, la barba que le erizaba la cara” (Borges 195). El odio a sí mismo surge al perder control. Obviamente, el infierno no es real pero para él esa obsesión es muy real. En este momento del cuento el personaje experimenta un estado de total vulnerabilidad. Él se enfrenta con la muerte y esto es una experiencia traumática. La combinación de la septicemia, las drogas y la proximidad a la muerte posible hace que él quiera librarse con la mente. El lenguaje que Borges utiliza es para que el lector no pueda diferenciar la realidad con los efectos delirantes ocasionados por

las drogas y la septicemia.

Una vez que es dado de alta del hospital, el propósito de Dahlmann es viajar a la estancia que había heredado de su abuelo en el sur. El viaje a la estancia inicia una secuencia donde es difícil determinar lo que es real y lo que es totalmente imaginado. ¿Salió del hospital o sólo lo hizo en su mente? El comienzo de esta secuencia se sitúa en la estación de trenes. Mientras esperaba el tren, Dahlmann entró en un café. En este café había un gato enorme que Dahlmann ya conocía. Dahlmann acaricia al gato y reflexiona sobre la naturaleza del tiempo. Dahlmann ha visto este gato en su pasado. El gato es parte de una realidad diferente que existió en un tiempo diferente. Aquí Borges vuelve a intercalar un cuestionamiento al tiempo que rige la realidad narrativa. Para Dahlmann, su contacto con el gato pareciera que fuera parte de otra realidad. Por eso dice: "...aquel contacto era ilusorio y que estaban como separados por un cristal, porque el hombre vive en el tiempo, en la sucesión, y el mágico animal, en la actualidad, en la eternidad del instante" (Borges 195). De esa manera se alude a un encuentro anterior pero no se ofrecen detalles. Esta idea de la eternidad del instante contra la sucesión es un ejemplo de la obsesión que Borges tiene respecto al tiempo. El tiempo es muy importante en la determinación de lo que es real y lo que es falso. La eternidad del instante no existe en realidad, pero para Borges sí. En los pensamientos de Dahlmann, el gato es parte de un tiempo que trasciende los límites de la realidad, un tiempo que une el presente con el pasado glorioso de sus ancestros.

Una vez en el tren, Dahlmann reflexiona sobre la separación entre la ciudad y los suburbios. El hecho de que la experiencia se refiera como una "visión" provoca a los lectores a pensar en el hecho de que todo el viaje en el tren es solamente una visión y nada más. Otro hecho que sugiere que todo es ilusorio es cuando Dahlmann se baja del tren en una parada antes de la estancia y la zona estaba completamente desierta. Cuando

llega al destino final del tren, en la estación antes de su parada, encuentra un restaurante, entra y comienza a leer las *Mil y una noches*. Mientras él estaba comiendo, un grupo de muchachones lo empiezan a burlar tirándole bolitas de migas de pan: “Dahlmann, perplejo, decidió que nada había ocurrido y abrió el volumen de las *Mil y una noches*, como para tapar la realidad” (Borges 197). Esta cita explica la tensión. El hecho que Dahlmann quiera tapar la realidad es interesante. Dahlmann usa el libro como un escudo para esconderse del mundo real. Las constantes insinuaciones que toda esta historia no está ocurriendo llevan a los lectores a preguntarse si la historia es verdadera o es una creación mental de Dahlmann. El personaje de Dahlmann se mueve entre el mundo real y el de los ancestros que él busca rescatar en su mente. El momento donde culmina esta secuencia es el relato de eventos que incluye el desafío de Dahlmann motivado por uno de los muchachones. Aunque Dahlmann es advertido por el patrón a que ignore a estos hombres porque sólo estaban borrachos, Dahlmann acepta el desafío. Un gaucho le da un cuchillo. Él prefiere morir a cuchillo como sus ancestros en vez de sucumbir a la septicemia en el hospital.

Cuando obtiene un cuchillo y se dispone a luchar, él se vuelve a referir al sanatorio con un sentido que hace que los lectores sospechen que está en el sanatorio y no tiene miedo de la lucha sino de romper las leyes del sanatorio: “Alguna vez había jugado con un puñal, como todos los hombres, pero su esgrima no pasaba de una noción de que los golpes deben ir hacia arriba y con el filo para adentro. No hubieran permitido en el sanatorio que me pasaran estas cosas, pensó. Salieron y si en él no había esperanza, tampoco había temor” (Borges 198).

También Dahlmann tiene pensamientos muy fuertes sobre su tiempo en el sanatorio. Al estar muy cerca de morir de septicemia él pasa mucho dolor y sufrimiento. A veces desea la muerte y la escena en la que entabla una lucha de cuchillo, puede

interpretarse como ser la manera ideal para morir, un sueño. A esta altura, el lector se cuestiona si la recreación del duelo entre Dahlmann y el compadrito es el resultado de un sueño: “Sintió, al atravesar el umbral, que morir en una pelea a cuchillo, a cielo abierto acometiendo, hubiera sido una liberación para él, una felicidad y una fiesta, en la primera noche del sanatorio, cuando le clavaron la aguja. Sintió que si él, entonces, hubiera podido elegir o soñar su muerte, ésta es la muerte que hubiera elegido o soñado. Dahlmann empuña con firmeza el cuchillo, que acaso no sabrá manejar, y sale a la llanura” (Borges 198).

Dahlmann es un argentino que busca conectarse con sus raíces, un pasado que le daba significado a su vida monótona. Hay una constante batalla entre los pensamientos y las ilusiones de Dahlmann y lo que le está ocurriendo en la realidad. Borges hace uso de las alusiones del tiempo y confunde las barreras de lo factible y lo soñado para hacer participar a los lectores en una lucha intelectual con ellos mismos, a fin de determinar qué en la historia es la verdad y qué es la fantasía. Es posible que Dahlmann se enfrente con la misma lucha interna que los lectores, pues él también debe someterse a la creatividad de Borges de pensar que las ilusiones son realidad.

En la narrativa hay una necesidad para una diferenciación de las dos formas del tiempo. Por un lado tenemos el relato de un personaje en el tiempo y, por otro, un relato inventado o atemporal que se inserta dentro del otro para darnos otro modo de interpretar los hechos. Tenemos la fusión de un relato que respeta nuestra experiencia del tiempo y otro que se construye fuera de él. Borges crea la confusión del tiempo aprovechando el estado de vulnerabilidad del personaje. La ausencia de restricciones de tiempo permite a los lectores formar su propia interpretación del relato.

## References

Borges, Jorge Luis. "El Sur." *Panoramas literarios América Hispana*. Ed. Teresa Méndez-Faith. New York: Houghton Mifflin, 2008.

## **I Want My Future to Be Different**

Jessica Gruber

Faculty Advisor: Dr. Seth Frechie

*Junior Jessica Gruber has crafted a insightful analysis of Mike Nichols' 1967 film, The Graduate. Employing an interdisciplinary approach to her subject, Ms. Gruber, an English major, has applied the methodologies of literary study to film media with surprising results. The generational divide that is director Nichols' focus is cast in an altogether new light, reclaiming contemporary relevance for this decades old film.*

Benjamin Braddock becomes disillusioned with his parents' shallow and materialistic life, causing him to question their values and subsequently, to seek meaning elsewhere, away from a life built upon "plastics." As a result, he refuses to go to graduate school or join the workforce. Instead, he finds his own fulfillment through the pursuit of Elaine and the romantic love he feels for her. To this end, Ben rejects the values and lifestyles of the insensitive and corrupt adults of his parent's age by running away to start a new life with Elaine. Such a portrayal of Ben in *The Graduate* showcases the widening generation gap that was occurring in 1967 when the film was produced between 1950's parents and their 1960's children.

The generation gap began to form when the children of the 1960's no longer looked to their 1950's parents as being ideal role models or as espousing the values and lifestyles these young people aspired to covet for themselves (Abrams, Bell & Udris, 2001). This is portrayed in *The Graduate* beginning with the first scene. Immediately, one realizes that Ben doesn't look up to his parents, nor does he want the life they are constantly encouraging him to pursue. For instance, Ben's parents are seen as heavy drinkers and as hypocrites because they espouse values they themselves don't follow (Holden, 1997). They desire that he either go to graduate school or, better yet, get a job

in the plastics industry. To this end, happiness for them is built upon an artificial industry making their world, in turn, artificial as well (National Public Radio, 2002). Ben further reinforces that he finds such a lifestyle unfulfilling and wants a different life for himself when he states, “I want my future to be different [from my parents’]” during his graduation party (*The Graduate*, 1967).

In addition to his parents being portrayed in a negative light, Mrs. Robinson is also shown as an adult figure who represents an immoral lifestyle. For instance, Mrs. Robinson, who is a married woman, initiates the affair. Ben tries several times to escape her trap before the affair is actually consummated, but Mrs. Robinson persists doggedly. In addition, she does not only commit adultery against her husband, but she seduces Ben by making him uncomfortable. For instance, she blatantly undresses in front of him even though he begs for her to stop. She manages to finally goad him into going through with the affair by challenging him, stating that if he’s afraid he’ll be “inadequate” they don’t have to go through with it (*The Graduate*, 1967). In this way, Mrs. Robinson constantly pushes Ben to engage in the immoral act for her own selfish purposes, and refuses to accept or even acknowledge the multiple ways he tries in the beginning to avoid the situation. In addition, Mrs. Robinson later threatens to tell Elaine about their affair if Ben refuses to stop seeing Elaine. Essentially, she is willing to hurt her own daughter and ruin Elaine’s happiness in order to accomplish her own goal. The way in which Mrs. Robinson consistently disregards the feelings of others—her husband’s, Ben’s, and Elaine’s—serves to depict her an immoral woman. Film critic, Stephen Holden (1997), even goes so far as to describe the older woman as a “monster.”

Such scenes in the beginning of the film, then work to show the audience that the adults are hypocritical and immoral and that their lifestyles are based upon artificial happiness. The adults’ supposed happiness is proved to be a fallacy when it is revealed

that Mrs. Robinson and her husband are not happily married; instead, they sleep in separate rooms and she is so unsatisfied that she must seek out attention from young Ben. Essentially then, they and their lifestyles are seen as materialistic and shallow, in part because they look for fulfillment in values such as financial success and sexual satisfaction which don't bring them happiness in the end. Mrs. Robinson in particular does not strive to foster a healthy marriage, nor does she cultivate fulfillment through romantic love. Also, she cares little about the feelings of Ben beyond keeping him placated so that he continues to meet her at the hotel. In this same way, Ben's parents want him to be successful financially in terms of a well-paying job, but at the expense of his happiness. Essentially, they do not care if their son is fulfilled through such an occupation. If Ben's lack of action is any indication that he doesn't want to pursue a career in plastics, his parents ignore it and instead continue to pressure him to do so. They don't consider for one moment that he might desire to find happiness by following a different path.

To this end, Ben rejects his parents' values by refusing to join the workforce or continue his education as they insist. He does this because he is afraid that following the path his parents are laying out for him, the path that both his parents and the Robinsons followed, will lead him to the same destination they arrived at: unfulfilled, although materially or financially successful, and stuck in an unhappy as well as unloving marriage. Instead, he chooses listlessly to waste his time by floating in the pool during the day and meeting Mrs. Robinson at night. His parents become quite upset at his behavior and attack him with questions concerning his plans for the future and demand to know what purpose his years in college have achieved because he seems to have put his life on hold. Ben doggedly refuses to give in to their demands and continues to loaf, suggesting that Ben lacks his parents' ambition, the ambition one needs to survive in a



plastic world.

In the same way that Ben's parents refuse to listen to his feelings concerning the future that he envisions for himself, so too do they disregard his concerns. For instance, Ben's father insists that Ben wear the scuba gear he received as a graduation gift and model it in front of a group of the Braddocks' friends. Ben continually tries to tell his father that he feels uncomfortable doing so, but each time Mr. Braddock interrupts him and goads him into stepping outside. Mr. Braddock also makes Ben feel guilty about his reluctance to show off his present by claiming, "They're all waiting for you, Ben" (*The Graduate*, 1967). It is in this way that the viewer can see, again, how Ben's parents disregard his emotions and desires. This also effectively shows their hypocrisy in that they are unwilling to value Ben's dreams, but are insistent that he follow the ones they deem important and have laid out for him. They continually push him to find a "greater purpose in life" by acquiring a job in the plastics industry, unconcerned that such expectations are "daunting" for Ben (A critical analysis of *The Graduate*, 2009). In addition, while Ben does give in to his father in the above-mentioned scene, he later refuses to accept the other plans that his parents try to foist on him.

It takes Ben longer to reject Mrs. Robinson and the affair than it took him to reject his parents and their expectations, but eventually he does that too, choosing to not continue an experience he describes as being as intimate as "shaking hands" (Dirks, 2008). For Ben, there is no fulfillment in the affair. To this end, one might argue that it is the lack of intimacy in the affair and also the demand that he enter into an artificial world that combine to make Ben seek fulfillment elsewhere—in something or someone more "real." This someone turns out to be Elaine Robinson. At first, Ben doesn't want to ask her out on a date, mostly due to Mrs. Robinson's request that he leave her daughter alone. His parents, though, continually pressure him to do so and, eventually, Ben

succumbs. In this way, he satisfies his parents in that he takes Elaine out, yet while he's on the date he tries to satisfy Mrs. Robinson as well by sabotaging the evening. In the end, however, he recognizes the value of Elaine and the importance of what she brings to his life, namely that she is the "first thing in so long that [he] like[s]" (Dirks, 2008). Once Ben realizes the romantic love he feels for Elaine is fulfilling, he springs into action. Gone is the man who floated aimlessly around his pool during the day, and in his place is a man who is willing to fight adamantly for the girl he longs to marry.

"Ben is roused to action by one thing only: his love for Elaine"; and for that love he is willing to stand up to Mrs. Robinson and her threats. He is even willing to tell Elaine about the affair before her mother does because he knows his honesty is the only chance he has to save the relationship (Holden, 1997). Ben also springs into action by deciding to pursue Elaine. To this end, the film shows him tracking her down at Berkley and begging her to marry him. The energy his parents felt he should have been putting into obtaining a job in plastics is instead applied to getting Elaine to be his wife. Ben even goes so far as to hunt her down at the church when he learns that she is marrying another man. Undeterred by any obstacle, Ben tricks the secretary into giving him the location of the church and runs the last few miles to the wedding when his car runs out of gas. In this way, he shows that he will stop at nothing to pursue Elaine (and subsequently, his dream).

When he arrives at the church, Ben is no longer scared of the adults present or the threats made by the Robinsons. Instead, he shows them how far he is willing to go in order to reject their lifestyle by physically fighting them off after grabbing Elaine from the arms of her new husband. He "saves" Elaine from following the path of her parents and whisks her out of the church, barring the door behind them with the crucifix. In this way, Ben is constructing a physical barrier between his parents' generation and himself,

and he is showing the adults in his life that he doesn't want to be like them: he is breaking with them by making a break for it. Finally, a line has been drawn between the generations and Ben literally walks away from that lifestyle and the unfulfilling outcome he knows it would create.

The final scenes of *The Graduate* clearly show Ben and Elaine rejecting their parents' life. They are made to fight physically for their own dream: not a job in plastics, but rather romantic love. Even after they barricade the adults in the church, however, the couple is still not free. They must literally escape from the adults' artificial world by jumping on a bus and heading off to some unknown location where they can begin their own life together on their own terms. It is here that they escape the jungle of their parents' world in pursuit of their own dreams, dreams that their adult parents do not understand or support (National Public Radio, 2002).

Thus, Ben, stirred to action by his love for Elaine, eventually gains the courage to reject his parents' values and demand his own happiness on his terms. His future after doing so, however, is unclear at the film's conclusion (Holden, 1997). One does not know if Ben's choice to run off with Elaine or, to be more specific, his decision to pick romantic love over all else, is successful. He has rejected the world of his parents, but is his world any better? Will romantic love really bring Ben happiness in the end, or will he also end up as a hypocritical and immoral individual? In this way, the film is one of a number of "youth culture" movies about...the generation gap" between the 1950's parents and their children (Cook, 2003, p. 854). *The Graduate* depicts this gap through the portrayal of Ben's rejection of his own parents' and the Robinsons' lifestyle and espoused values. However, the film does not show the fallout or the result of this break having occurred. One is left wondering if the 1960's generation will end up any happier than are their predecessors after all.

## References

- Abrams, N., Bell, I., & Udris, J. (2001). *Studying film*. London: Hodder Arnold.
- A critical analysis of *The Graduate. Pins and Needles*. (2009). University of North Carolina at Chapel Hill. ([www.unc.edu/~jbenton/Graduate\\_Analysis.html](http://www.unc.edu/~jbenton/Graduate_Analysis.html)[April 6, 2009.]).
- Cook, D. A. (2003). *A history of narrative film*. Boston: W.W. Norton & Company.
- Dirks, T. (2008). *The Graduate* (1967). *Filmsite.org*. ([www.filmsite.org/grad.html](http://www.filmsite.org/grad.html)[March 2, 2009]).
- National Public Radio. (2002, December 9). *The Graduate*. ([www.npr.org/programs/morning/features/patc/graduate/index.html](http://www.npr.org/programs/morning/features/patc/graduate/index.html)[March 2, 2009]).
- The Graduate*. (1967). Dir. Mike Nichols. Perf. Anne Bancroft, Dustin Hoffman, Katharine Ross, William Daniels, Murray Hamilton, and Elizabeth Wilson. DVD. Embassy Pictures.
- Holden, Stephen. (1997, February 19). What's that you say now, Mrs. Robinson? *New York Times*. ([www.writing.upenn.edu/~afilreis/50s/graduate.html](http://www.writing.upenn.edu/~afilreis/50s/graduate.html)[March 2, 2009]).

## **Análisis del poema “Explico Algunas Cosas”**

Heather Peters

Faculty Advisor: Dr. Raquel Green

*Heather Peters, a Spanish major in the Romance Languages and Literatures Department at Cabrini College presented an original study on the Chilean poet Pablo Neruda, titled, “Análisis del poema ‘Explico algunas cosas’.” The paper explores Neruda’s poetic voice as a construct that serves not only to give testimony of the atrocities committed during the Spanish Civil War, but also to remind new generations of the enduring power of the poetic word. The paper was written in the fall 2008 as part of the requirements for the Survey of Latin American Literature I course. Miss Peters presented her work in Spanish at the Undergraduate Research Symposium at Cabrini College in April 2009.*

### **Introducción**

Durante la época de la Guerra Civil de España, muchos artistas se vieron afectados profundamente por los acontecimientos. El poeta chileno Pablo Neruda, pasó muchos años en España durante este difícil proceso y los resultados de este conflicto tuvieron un efecto profundo en él. Fue durante estos años que Neruda perdió algunos de sus amigos íntimos. En su famoso poema “Explico Algunas Cosas,” el poeta chileno reflexiona sobre estos hechos y se refiere a Federico García Lorca, quien fue asesinado por los franquistas. La Guerra Civil fue una época de muchas pérdidas, y Neruda quería que los opresores supieran que el mundo tenía una manera de hacer justicia. El título del poema de Neruda puede sintetizar una tesis. Hay muchas maneras de deconstruir este poema.

## **Análisis del Poema**

Una manera es ver cómo el poema puede ser dividido en cinco partes que cambian de tono. En la primera parte se establecen las preguntas que él contestará luego en el poema. La segunda parte es la descripción del lugar que él vivió en España. La descripción es inocente, tranquila y pacífica. En la tercera parte hay ya un cambio. Aquí es donde Neruda invoca los nombres de sus amigos y él comienza a demostrar su sentimiento de pérdida. En la cuarta parte, el poema expresa la frustración de la voz poética. Las cosas han cambiado. Los verbos que Neruda utiliza cambian de unos que son utilizados pasivamente a otros que son utilizados activamente. Los verbos como “fatigar” y “arder” y “devorar.” Su lugar, su barrio y su hogar han pasado de ser un lugar pacífico y armónico a un lugar de ira, sufrimiento y dolor. En la quinta parte, el poema comienza a expresar el estado verdadero de España durante la guerra. Todo el resentimiento de Neruda queda claro. Neruda muestra la tragedia de los acontecimientos de la guerra. El poeta habla sobre los incendios, los fusiles, la sangre y la muerte. Las descripciones llegan a ser abiertamente gráficas.

Otra manera de deconstruir el poema es verlo como una descripción del paraíso y del infierno. En la primera estanza, el poeta habla de las flores y los pájaros, de las campanas y los árboles, de la hermosura de su casa, y de los niños y los perros que jugaban en la calle. El poeta describe este mundo como si fuera su propio paraíso. Hay un sentimiento que se traslada a lo blanco y brillante. En la cuarta estanza del poema, las descripciones son oscuras, imperdonables y dolorosas, para connotar la entrada al infierno. La voz poética explica cómo se marchitaron las flores y la pérdida de sus amigos. Neruda pregunta “Raúl te acuerdas? Te acuerdas, Rafael? Federico, te acuerdas? Debajo de la tierra, te acuerdas de mi casa con balcones en donde la luz de junio ahogaba flores en tu boca? Hermano, hermano!” (Neruda, 2008, p. 182). El poeta

está gritando por sus amigos perdidos. En este espacio transformado, el sol es frío ahora y los fuegos ya incendiaron todo. El yo poético describe cómo la muerte se apoderó de las vidas de muchos niños que jugaban en la calle. A los opresores y los enemigos se los describe como demonios “Chacales que el chacal rechazaría” y “víboras que las víboras odiaron!” (Neruda, 2008, p. 183). Neruda antropomorfiza a estos animales porque viven por oportunidad e indiferencia, es decir son los que viven a costa de las vidas débiles. De esta manera, el poeta describe a los enemigos como si fueran figuras nefastas. El lugar es ahora el infierno.

Otra manera de deconstruir este poema es trazando la manera que el poeta se dirige a la audiencia. El poema puede ser estructurado en tres partes. En el principio, él comienza por hablar a un tipo de receptor y luego se dirige a otro receptor y finalmente a un tercero. Al principio, el poeta se dirige al lector en una manera inocente. El poeta describe lo que era su vecindario antes de la guerra, como si él estuviera mostrándonos un álbum de fotografías. Parecería que la audiencia estuviera destinada a ser como las personas inocentes, como nosotros. La persona poética habla en una voz amistosa. En la segunda parte, él comienza a hablar de los amigos que él perdió. Ahora el poeta pregunta a sus amigos ausentes si ellos recuerdan como había sido el vecindario antes de que todo cambiara. En la tercera parte, la voz poética se dirige indirectamente a los opresores. El tono del poema se torna dramático y llega a ser lleno de ira, acusación y odio. El “yo” habla directamente a las personas que son responsables de la destrucción de su vida, su casa y sus vecinos. Él comienza con el ambiente nuevo del vecino y describe las atrocidades que vio. A partir de aquí se comienza a describir a los opresores. A este punto, el tono, la descripción y las palabras escogidas llegan a ser imperdonables y acusativas. El yo poético dice lo que él piensa de los enemigos y los llama “Generales Traidores” (Neruda, 2008, p. 184). También desafía a los enemigos para delatar lo que

hicieron, su destrucción de vecindarios, hogares y gente. Él los invita a mirar la sangre en las calles. Entonces, les dice, “pero de cada niño muerto sale un fusil con ojos, pero de cada crimen nacen balas que os hallarán un día el sitio del corazón” (Neruda, 2008, p. 184). Él está amenazándolos que la gente logrará desquitarse.

El tema central que se presenta en el poema es el tema del cambio, pero la permanencia de la memoria. El tema del cambio es característico del período del posmodernismo. Este período es conocido por su relación a los cambios profundos que sufrió el mundo. Aunque España no es su país natal, el poeta se sintió conectado al país en una manera muy fuerte. Él llegó a sentirse cercano a muchas personas y desarrolló muchas amistades. Él conoció a su segunda esposa allí. Está claro que Neruda se sintió muy afectado por los acontecimientos que pasaron en este país durante la Guerra Civil. El poeta presenta una tesis en una manera engañosa. El poema parece ser un testimonio a los acontecimientos atroces de la Guerra Civil. Pero es más complicado que esto, ya que el poema comienza con una explicación de los acontecimientos, pero casi sin mencionarlos en ninguna parte, el poema llega a ser un desafío abierto a los opresores, algo que es inesperado para el receptor. A este punto nos toma por sorpresa porque el poema comienza lo que va a ser una descripción solamente pero, por fin, llega a ser un ataque a los enemigos. El poema explica muchas cosas, el estado de España antes y después de la Guerra Civil, la felicidad y la tristeza. Además se enfrenta a los opresores y a nosotros para tratar estos temas. Cuando dice, “¡Venid a ver la sangre por las calles, venid a ver, la sangre por las calles, venid a ver la sangre, por las calles!” (Neruda, 2008, p. 184), el poeta está exigiendo que los opresores miren lo que ellos hicieron y, lo que es más importante, exige que todo el mundo no olvide nunca lo que pasó allí. De ahí que el poema se transforme también en una afirmación de la memoria del pueblo. Él dice que la guerra no se ha podido olvidar y no se podrá olvidar, el sufrimiento continúa. El poeta se



transforma en el defensor de todos los que sufrieron en la guerra. Él dice que los opresores pagarán de alguna manera por lo que ellos han hecho. El poema en sí se transforma en símbolo de lo perecedero de la memoria que queda para siempre vigente a través de la palabra.

### References

Neruda, P. (2008). "Explico algunas cosas." In T. Méndez-Faith (Ed.), *Panoramas literarios América Hispana* (pp. 182-184). New York: Houghton Mifflin.

**Una Mirada a la vida de Miquel de Cervantes a través de la caracterización: A Glimpse into the Life of Miguel de Cervantes Through Characterization**

Kelly Smith

Faculty Advisor: Dr. Cynthia Halpern

*The paper, “Una mirada a la vida de Miguel de Cervantes a través de la caracterización” was written by Kelly Smith, a Spanish major in the Romance Languages and Literatures Department at Cabrini College, as a part of the requirements for the Honor’s course, Don Quixote and the Art of Imagination in the fall 2008. It is an original study of several characters found in Miguel de Cervantes’s masterpiece Don Quixote. Miss Smith compares these characters to people in the author’s personal life. Miss Smith presented her findings in Spanish at the Honors Symposium in March 2009 at Neumann College in Aston, Pennsylvania, and in April 2009 at Cabrini College’s Undergraduate Research Symposium.*

La novela de Miguel de Cervantes, *Don Quijote*, es más que una novela sobre el sueño de un hombre que quiere hacerse el caballero andante de La Mancha. Hay más en la novela de Miguel de Cervantes que las palabras y las oraciones que llenan cada página. Muchos lectores no pueden comprender el significado verdadero de la novela sin la comprensión de la historia personal de Cervantes. Por toda la novela, Cervantes incorpora una parte de su vida personal que se encuentra en los personajes que él inventa. La vida personal de Cervantes está entrelazada con las personalidades y las historias de los personajes de la novela. Cervantes representa discretamente los temas y las luchas en su vida por sus personajes y sus vidas. En la primera parte de la novela, Cervantes utiliza cinco personajes para representar los temas de su vida. Los cinco personajes que representan un tema personal de la vida del Cervantes son: don Quijote,

el cautivo, Lothario y Camilla, y Maritornes. Todos los personajes dan a los lectores una vislumbre en la vida personal de Cervantes.

Cervantes utiliza al personaje principal, don Quijote de la Mancha, para representar los temas importantes en su vida. Este personaje de don Quijote se relaciona frecuentemente con la vida de Cervantes. La primera conexión importante entre Cervantes y el personaje de don Quijote es que los dos hombres son soldados o caballeros dedicados a su profesión. Hay una relación distinta con la dedicación de Cervantes como soldado y la dedicación de don Quijote como caballero andante. El estudio de Carlos Fuentes en la edición del *Quijote* de Tobias Smollett (2001) dice que “...we have very little information touching the transactions of his [Cervante’s] life...we learn that he was a chamberlain to cardinal Aquaviva in Rome, and followed the profession of a soldier” (p. 10). Aún más, se dice que Cervantes “...lost his left hand by the shot of an arquebus” (p. 10). Igualmente, don Quijote expresa su dedicación como caballero andante en la novela de *Don Quijote*, “[it was necessary for don Quixote], both for the sake of his honor and as a service to the nation, to become a knights errant and travel the world with his armor and his horse to seek adventures and engage in everything he had read that knights errant engaged in, righting all manner of wrongs and, by seizing the opportunity and placing himself in danger...” (p. 21). Esta relación entre Cervantes y don Quijote no es la única conexión entre la vida del autor con la del personaje principal de la novela.

Irónicamente, ninguno de los dos hombres recibió una recompensa para sus obras grandes como soldado y caballero. Como resultado, Cervantes y don Quijote eran muy pobres. Ninguno de los dos hombres tenía la seguridad financiera para pagar sus deudas tampoco. Cervantes nunca recibió la recompensa justa por su novela popular de *Don Quijote*. El estudio de Carlos Fuentes explica que Cervantes no podía satisfacer sus

deudas. Esto causó muchas dificultades para él, "...we cannot be surprised to find his [Cervante's] finances in a little time exhausted..." (Smollett, 2001, p. 16). También Fuentes nos dice que, "...the poverty of Cervantes had increased to such a degree of distress..." (p. 24). Muchos atribuyen la pobreza de Cervantes y las dificultades que tenía por toda su vida a la ascendencia judía de su familia. Durante el período barroco, había mucha discriminación y tener la sangre limpia tenía gran importancia. También, don Quijote nunca tenía dinero para satisfacer sus deudas. Él tenía muchas dificultades parecidas a las de Cervantes. Por ejemplo, don Quijote durmió una noche en una venta. Él nunca le pagó al propietario de la venta por su visita. El propietario de la venta estaba muy enojado con don Quijote, "[The] greatly displeased innkeeper, who warned him that if he did not pay, he would collect his money in a way [Quixote would regret]" (Cervantes, 2003, p. 121–122). Don Quijote no es el único personaje que representa la vida de Cervantes.

Otro personaje que representa la vida de Cervantes es el personaje del cautivo. El cautivo representa una parte importante y significativa de la vida de Cervantes porque nuestro autor era un cautivo en Argel, "...[Cervantes] was unfortunately taken by a Barbary corsair and conveyed to Algiers...and remained a slave for the space of five years..." (Smollett, 2001, p. 12). Parecido a Cervantes, el cautivo estaba encarcelado por los turcos en Argel por muchos años. En la novela *Don Quijote*, el cautivo relata su historia como cautivo en Argel, "...I spent my life, locked in a prison or house that the Turks call a bagnio" (Cervantes, 2003, p. 343). En la novela, el cautivo hace referencia a otro cautivo con el nombre Cervantes durante su encarcelamiento en Argel. El cautivo describe como los dueños de los cautivos les pegarían. Pero los dueños nunca pegarían al hombre con el nombre de Saavedra (el apellido de Cervantes). De una manera, Cervantes se jacta sobre su encarcelamiento y su valentía, "...The only one who held his

own with [the master] was a Spanish soldier named something de Saavedra, who did things that will be remembered by those people for many years...yet his master never beat him..." (Cervantes, p. 344). Aquí, Cervantes alude a su encarcelamiento como un cautivo por el cuento del personaje del cautivo en la novela. Cervantes inserta elementos de su propia vida en esta historia de la novela suya.

También, Cervantes deja que los lectores se involucren a sí mismos en su vida. Él desarrolla e incluye a los personajes de Lothario y Camila en su novella en una de sus historias interpoladas. El problema entre Lothario y Camila está relacionado con un problema en la vida de Cervantes. Lothario y Camila tenían una relación secreta. Lothario decidió, con la insistencia de Anselmo, tener una relación con la mujer Camila, la esposa de su mejor amigo Anselmo porque Anselmo quería probar la lealtad de su mujer. Lothario y Camila pasaban mucho tiempo escondiendo sus relaciones de todas las personas; especialmente Anselmo porque irónicamente se enamoraron al fin de todo, "All that Camilla could do was implore Leonela (her maid) not to say anything about her mistress's affair to the man she said was her lover, and to keep her own secret so that it would not come to the attention of Anselmo" (Cervantes, 2003, p. 295). Sin embargo, el plan de Lothario y Camila falló. Eventualmente, Anselmo descubrió la relación. Cervantes tenía una situación semejante a Lothario y Camila. Cervantes tenía una aventura amorosa con la mujer Ana Franca de Rojas. Cervantes tenía que esconder la relación amorosa que tenía con Ana Franca de Rojas. Durante el mismo tiempo, Cervantes estaba comprometido con una mujer Catalina de Palacios Salazar Vozmediano, "The affair with Ana Franca occurred in January or February...[it] was clearly something that Cervantes preferred to keep a secret from his wife-to-be" (McCrary, 2002, p. 115). Sin embargo, a la diferencia de Lothario y Camila, Cervantes tenía una hija ilegítima con Ana Franca de Rojas; el nombre de su hija era Isabel. No

obstante, Cervantes incluye una parte de su vida personal en su novela en el cuento de Lothario y Camila. Hay un personaje más que Cervantes utiliza para desenvolver una parte de su vida personal.

El último personaje que Cervantes utiliza como ejemplo de su vida es el personaje de Maritornes. En la novela de *Don Quijote*, Maritornes se describe como una mujer con poca belleza. Ella tiene, "...a broad face, a back of the head that was flat, a nose that was snubbed, and one eye that was blind..." (Cervantes, 2003, p. 109). Sin embargo, con ensueños de caballería don Quijote le ve como una mujer muy bonita en vez de una prostituta poco atractiva, "Her tresses, which were rather like a horses' main, [don Quijote] deemed strands of shining Arabian gold...[don Quijote] depicted her in his imagination as having the form and appearance of another princess..." (Cervantes, p. 113). También, Maritornes trabajaba en la venta que don Quijote visitaba a veces. Irónicamente, Maritornes puede ser comparada con Ana Franca de Rojas. Ana Franca de Rojas trabajaba en una venta como Maritornes también. McCrory describe a estas personas que trabajaban en las ventas así, "...practicioners of other 'vile' and 'lowly' trades...accounts of the period show that inns were notorious for their 'filth', vermin, noise, and their hostile clientele and owners" (McCrory, 2002, p. 114). Los lectores pueden deducir que Ana Franca de Rojas es como el personaje de Maritornes. Las dos mujeres trabajaban en una venta. Los lectores pueden deducir que Ana Franca de Rojas era poco atractiva como Maritornes también. Sin embargo, es posible que Cervantes no se preocupaba de la belleza de Ana Franca de Rojas igual que don Quijote no se preocupa de la belleza de Maritornes.

Los lectores pueden observar por los cinco personajes de la novela de *Don Quijote* que la novela es más que una novela sobre un caballero andante y aventuras de caballería. Todos los personajes en la novela son unas representaciones de personas

verdaderas de la vida personal y problemática de Cervantes. Por los cinco personajes, Cervantes puede expresar secretamente sus propios sentimientos y permite que los lectores sepan algo de los temas y las dificultades durante su vida. Los lectores de la novela no pueden apreciar completamente la novela hasta que ellos absorban los detalles de la vida personal de Cervantes. Con este conocimiento enriquecido, los lectores pueden meterse completamente en la novela y pueden darse cuenta del significado oculto y verdadero de la novela *Don Quijote* y el caballero andante de La Mancha.

### References

- Cervantes, Miguel de. (2003). *Don Quixote*. E. Grossman (Trans.). New York: Harper Collins.
- McCrary, D. P. (2002). *No ordinary man: The life and times of Miguel de Cervantes*. London: Peter Owen.
- Smollett, T. (Trans.). (2001). "The Life of Cervantes." In *Don Quixote*, by Miguel de Cervantes (pp. 7–29). New York: The Modern Library.

LIFE & PHYSICAL  
SCIENCES



## **DNA Barcoding of Crayfish Species**

Zach Berman, Emily K. Bongiorno

Faculty Advisor: Dr. David Dunbar

*Serving as their Undergraduate Research Advisor, I have had the privilege of getting to know both Zach and Emily quite well over the last several years. About a year and a half ago, Zach asked me if he could engage in any research projects that are focused on molecular genetics. At the time, I had no projects in mind for Zach, but told him I would consider him for any future research projects. About this time, I stumbled upon an innovative molecular genetics technique called DNA barcoding. DNA barcoding involve the determination of an animal species at the DNA level by the DNA sequence of an animal's mitochondrial C Oxidase gene. Since DNA barcoding is such a new field and my lab is very small, I was concerned that we were ill equipped to take on a project of this magnitude.*

*About the same time that Zach indicated that he would be excited to take on a DNA-barcoding project, Emily finished her summer research on using macroinvertebrates (stream insects) on Crabby Creek. Macroinvertebrates are a proven indicator species of stream health. Because of both Zach and Emily's interests, we decided to conduct our DNA-barcoding studies on macroinvertebrates and other aquatic organisms such as crayfish. No one has ever DNA-barcoded macroinvertebrates and there was very little literature on protocols for DNA-barcoding crayfish as well. Within the course of a year's time and with much perseverance, both Zach and Emily, largely on their own, developed DNA-barcoding protocols and successfully barcoded several macroinvertebrate species as well as several crayfish species. For undergraduates to develop their own research protocols and conduct cutting-edge research is an expectation of graduate students, not undergraduate*

*students!*

*As a result of all these efforts, both Zach and Emily presented their DNA-barcoding work at the 2007 National Conference on Undergraduate Research Symposium and coauthored a paper published in the NCUR Proceedings Journal. Emily also presented her Crabby Creek macroinvertebrate work at the Pennsylvania Capitol Poster on the Hill event in Harrisburg during April of 2008.*

*As you can see, both Zach and Emily have already contributed significantly to an important project in DNA barcoding in developing protocols for barcoding aquatic organisms. Both Zach and Emily plan on graduate studies after receiving science degrees at Cabrini College. I have the utmost confidence that both Zach and Emily have what it takes to become great, bench scientists someday.*

### **Abstract**

DNA barcoding is a relatively new molecular method for species identification. The procedure has been used successfully in hundreds of thousands of species and is a highly important tool to use in conjunction with current taxonomic procedures for species identification. Using an extraction method and PCR, a section of the mitochondrial cytochrome c oxidase I (COI) gene is sequenced and analyzed. The COI gene codes for the cytochrome c oxidase protein, which participates in the electron transport chain. The gene itself is an ideal sequence for barcoding because it is highly variable and is contained in the mitochondrial genome of almost all eukaryotes. This procedure is currently being performed on several species of crustacean in the genus *Orconectes*. It should be possible to distinguish the sequence differences between *Orconectes immunis* and *Orconectes compressus* using universal primers to amplify the

COI sequence. The sequence of one species has been found and it is a match to the sequence for the COI sequence *Orconectes compressus* found in GenBank. This sequence has not yet been submitted to the Barcode of Life Data Systems (BOLD). This database is dedicated to current species information and identification, collection and analysis based on the new method of DNA barcoding. By submitting the resulting to BOLD the database will be able to grow as a taxonomic reference to be used by various fields of study. Acquiring these accurate species identifications is crucial to understanding the nuances and complexities of nature.

**Keywords: DNA barcoding, COI, BOLD**

## **Introduction**

With the explosion of molecular biology in today's society, taxonomic methods are becoming more diverse with the addition of DNA barcoding. Because species identification is time consuming and requires a highly trained and specialized individual, the old-fashioned taxonomic identification practices are being amended. Identifying an organism at the species level is very difficult and morphologies among species can make accurate identification challenging. Depending on an organism's stage of life, it can resemble other species entirely, and because some species are only found when they resemble closely related species, the process is more challenging still.<sup>1</sup> It is for these reasons that molecular methods for species identification have become more commonly used.

DNA barcoding is a method used for species identification that depends on a sequence from the cytochrome *c* oxidase I (COI) gene found in the mitochondrial genome of almost all eukaryotes.<sup>2</sup> With the sequence differences in this region, a

molecular barcode can be produced. This method for species identification was devised by Herbert et al. (2003).

The mitochondrial genome is very small consisting of a 16 kb circular genome. The genes found in the mitochondrial genome are used primarily for ATP synthesis via cellular respiration. The mitochondrial genome has 2 genes coding for rRNA, 22 genes coding for tRNA, and 13 genes coding for proteins associated with cell respiration and the synthesis of ATP.<sup>3</sup> The COI gene used in this study is a gene coding for a protein associated with the electron transport chain. The COI sequence is highly conserved in a matter of function. Being a protein-coding gene, the COI gene has accumulated mutation, but not enough to alter its function.

The Consortium of the Barcode of Life (CBOL) was formed in 2004 and is comprised of over 150 institutions in 45 countries. The goal for the DNA barcoding initiative is to have barcoded all known species of fish and birds by 2012<sup>4</sup> and have 500,000 species barcoded by the year 2014.<sup>5</sup> CBOL has constructed a database, the Barcode of Life Data Systems or (BOLD), to store the DNA barcoding records. For submission to BOLD, 10 members of the same species have to be barcoded to compare sequences among members of the same species.

DNA barcoding is a very heated topic among scientists. Some think that it will seek to replace standard taxonomic methods.<sup>6</sup> This is not the case because DNA barcoding relies heavily on previously obtained taxonomic data. This data has been collected by ways of morphology among other methods.<sup>7</sup> This idea supports the notion of using integrative taxonomy. It is seen as an “irresponsible” move using one sequence to identify all life especially because its capability to accomplish this goal is questionable. Some believe that more species need to be discovered before barcoding can be used to supersede any taxonomic method. If used as an integrative method in

conjunction with taxonomy, DNA barcoding has the potential to yield more conclusive and pragmatic finds.<sup>8,6</sup>

DNA barcoding has led to several discoveries. For instance, the species previously thought to be *Astraptes fulgerator* was shown to be 10 different butterfly species, and it is likely that it will prove to be more. DNA barcoding has yielded more surprises than just new species. In addition to new species identification, it has shown that there is a surprisingly smaller amount of variation than scientists previously expected within some species, including *A. fulgerator*.<sup>9</sup>

DNA barcoding has many uses in several different industries. Rudnick, Katzner, Bragin, and DeWoody (2007) have developed a new technique for bird identification using restriction fragment length polymorphism (RFLP) analysis. This method has been tested for use in the food industry mainly for its ability to identify fish species that were grouped incorrectly and priced unfairly for restaurant use.<sup>10</sup> In other areas of study, DNA barcoding might be useful in species identification used in biological assessment of the environment. In cases in which organism such as macroinvertebrates are used to judge the quality of streams, having the correct species data might prove beneficial for ecological assessment.<sup>11</sup>

This study will focus on the DNA barcoding of the crayfish species *Orconectes immunis* and *Orconectes compressus*. *O. immunis* has been previously barcoded and submitted to the BOLD Systems. This species will serve as a control sample. *O. compressus* has not been barcoded, but the sequence for the COI region has been submitted to GenBank. It is thought that comparing two similar species in the same genus will give a better insight for the DNA sequence of a species. For this study, a universal primer set was selected so that the potential for protocol versatility within several species is possible.

## Materials and Methods

### *Tissue Isolation*

Ten members of the crayfish species *Orconectes compressus* were ordered from the company Living Aquatics while 10 members of the species *Orconectes immunis* were obtained through Carolina Biological. Before being sacrificed, crayfish species were stored separately in aquariums and fed a high-protein diet of sinking pellet fish food. Crayfish species were sacrificed via decapitation of the crayfish ¼ inch behind the eyes and stored in 95% ethanol. After sacrificing the crayfish their claws were removed and stored in 95% ethanol. Using sterile technique, muscle was taken from the claw of *O. immunis* and from the tail of the smaller species, *O. compressus* because these locations are known for their high concentration of mitochondria that would help to yield more mtDNA.

### *DNA Extraction*

Extraction of DNA was carried out using the Aqua Pure Genomic DNA kit. About 2mm<sup>3</sup> of the muscle sample was left to air dry for about 5 minutes and then added to a 1.5ml microfuge tube. 300µL of the Genomic DNA lysis solution was added and the sample was ground up using a pair of tweezers. The tube was incubated at 65°C for 45 minutes in a hot water bath and throughout this step was occasionally inverted. To precipitate the proteins, the lysate was cooled to room temperature before 100µl of the protein precipitation solution was added. It was vortexed for 20 seconds and centrifuged

at 13,000 rpm for 3 minutes, after which the proteins formed a tight pellet. The supernatant containing the DNA was poured into a new 1.5ml tube containing 300µl of 100% isopropanol. 1µl of glycogen was added and the solution was mixed by inverting several times. Again, the tube was centrifuged at 13,000 rpm for 1 minute until the DNA formed a tight blue pellet. The supernatant was poured off and the tube was drained on a clean paper towel. 300µl of 70% ethanol was added and the tube was inverted several times to wash the pellet. The solution was centrifuged at 13,000 rpm for 1 minute and the ethanol was poured off slowly, leaving the tight blue pellet behind. The tube was drained on a clean paper towel and allowed to air dry for 30 minutes to 1 hour. To rehydrate the DNA, 50µl of DNA hydration solution was added to the pellet and the system was incubated at 65°C for 30 minutes in a hot water bath. The solution and pellet was vortexed at 5 seconds to mix and stored in a -20°C freezer.

### *COI Amplification*

The COI sequence was amplified via PCR. The following reagents were added to facilitate the PCR reaction: 5µl of 10x Taq Buffer, 0.25 µl of dNTPs, 0.5 µl of the 3' COX1 primer, 0.5 µl of the COX1 primer, 0.25 µl of Taq Polymerase, 1 µl of the DNA sample, and 42.5 µl of deionized water for a total reaction of 50 µl. The primers used were COX1 5' (5'-GGTCAACAAATCATAAAGATATTGG-3') and COX1 3' (5'-TAAACTTTCAGGGT GACCAAAAATC-3'). The PCR was run with the following parameters: 1 cycle at 94°C for 1 minute, 30 cycles at 94°C for 1 minute, 40°C for 1 minute, and 72°C for 1 minute, the last cycle is a for 3 minutes at 72°C. After the PCR the 5 µl of sample was then run out on a 2% agarose gel with 1 µl of loading dye. The samples were run against a 100bp DNA ladder. The samples were run at 100 Volts for

30–40 minutes and then visualized on a Gel Doc.

### *Cloning Reaction*

Using a TOPO cloning reaction, the COI sequence was added to a plasmid that was grown in chemically competent *Escherichia coli*. The reaction, made up of 2µl of the PCR product containing the DNA, 1µl of a salt solution, 2µl water, and 1µl of the TOPO vector, was added to the thawed *E. coli* and incubated on ice for 30 minutes. The cells were heat-shocked for 30 seconds in a hot water bath at 42°C. The samples were transferred to ice and 250µl of S.O.C. media was added. The samples were placed in the shaking incubator for 1 hour. Next, 50µl of the transformation product was spread on a plate, containing LB/AMP media that had been warmed. The plates were incubated at 37°C overnight.

### *DNA Purification*

Purification of the plasmids was accomplished using an automated Mini-Prep 96<sup>TM</sup> machine from MacConnell Research that was able to purify the plasmid directly from the bacterial culture. Liquid cultures were prepared using sterile technique to add *E. coli* to 1.5ml Magnificent broth. 1µl of ampicillin was added for each milliliter of broth. The liquid cultures grew overnight in a shaking incubator at 200rpm at 37°C. The liquid cultures were pipetted in their entirety in to the wells of a cassette containing the lysis comb. The lysis tablets were added and using a swishing motion, the bacteria were lysed by the enzymes in the comb and tablet that also acted to destroy RNA, proteins and the cellular membranes. The samples were allowed to lyse for 15 minutes. A



standard plasmid purification program was selected and ran for 70 minutes, during which electrophoresis was used to separate the plasmid from the degraded cellular material. The plasmids run to the end of the separation gel and the electroelution stage begins. The DNA collects as a film on the filtration membrane. During the draining step, the buffer is removed and the DNA becomes unattached to the membrane. The DNA was then removed from the wells on the opposite side of the cassette.

#### *Verification of COI Uptake by Plasmid*

Using a restriction digest, the uptake of the COI region by the plasmid, and subsequently the bacteria was tested. EcoR1 is an endonuclease that creates sticky ends with 5' end overhangs and it proved useful in this step. The resulting DNA was then run with a loading dye and a 100bp ladder on a 2% agarose gel and visualized on a Gel Doc.

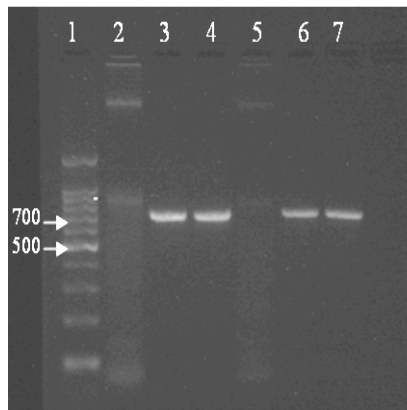
#### *DNA Sequencing and Analysis*

Purified plasmid DNA and T7 primers in a Tris buffer solution pH 8 were sent to the University of Maine DNA Sequencing Facility. Sequences were generated with an ABI 3730 Capillary Sequencer using a T7 sequencing primer.

## **Results**

Experimentation yielded results inconsistently because of the nature of the project; however, results that were found seem to state conclusively that sequencing the COI region shows potential for use as a species identification method. The theory that

the highest yield of mDNA would be found in the tail and claws was shown to be accurate because of the greater need for ATP in these cells. Samples from the tail or claw of the crayfish yielded much more DNA that could be visualized on a Gel Doc. The multistep, DNA-extraction procedure using the Aqua Pure Genomic DNA kit was much more reliable than other methods and our results show a high yield of genomic DNA. Figure 1 shows the genomic DNA of two samples from the *O. immunis* species in lanes 2 and 5. The COI region was also amplified via PCR successfully and can be seen in Figure 1 as well in its correct location, between 700 and 800 base pairs.



*Figure 1.* Genomic DNA and amplified COI region. Samples 101 and 102 (*O. immunis*) were amplified via PCR. The results were visualized on a 2% agarose gel. The first lane contains a 100 bp DNA ladder. Lanes 2 and 5 contain genomic DNA from samples 101 and 102, respectively. Lanes 3 and 4 have the COI sequence amplified from colonies from sample 101. Lanes 6 and 7 have the COI sequence amplified from 2 colonies from sample 102. The COI sequence is between 700 and 800 base pairs.

The COI sequence of the all of the *O. compressus* species was also successfully amplified with PCR. Nine out of the 10 samples shown in Figure 2 shows a noticeable band around 700 bp.

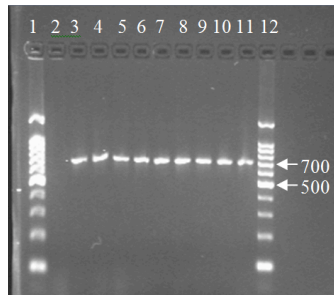
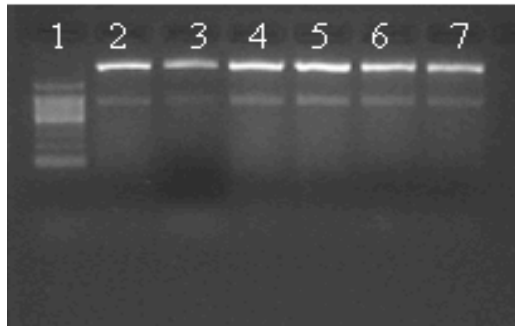


Figure 2. Amplified COI region of *O. compressus*. Samples 11–20 (*O. compressus*) were amplified via PCR using primers to amplify the barcoding region of the COI gene. The results were visualized on a 2% agarose gel. The gel indicates that the COI sequence that was amplified is between 700 and 800bp.

The transformations of *E. coli* with the plasmid containing the COI sequence showed poor transformation efficiency because few, if any, colonies grew after one try. Despite this, samples that showed growth were purified and the resulting plasmid samples were digested with *EcoR*I to verify the presence of the COI sequence within the plasmid. Figure 3 illustrates that the plasmid containing the COI sequence from both crayfish species has been taken up by the TOPO vector.



*Figure 3.* Restriction digest of TOPO plasmid containing COI sequence. The successful amplification of the COI sequence and incorporation into the TOPO cloning vector is shown. A restriction digest was performed to confirm the presence of the COI sequence in transformed *E. coli*. It shows sequence amplification of COI in sample 8 from *O. immunis* (lanes 2–4) and sample 13 from *O. compressus* (lanes 5–7).

Sequence results were obtained from the University of Maine DNA Sequencing facility with only one of five submitted samples showing readable, reliable, DNA-sequencing results. The DNA showed impurities that would need correction in order to be read. The sample that was able to be sequenced was sample thirteen from *O. compressus*, which was 725 base pairs in length, an encouraging result because the DNA gel showed an estimated length between 700 and 800 base pairs. The DNA sequence from the sample was run through the nucleotide BLAST database on GenBank. This sequencing resulted in 98% homology to an already existing sequence for *O. compressus*. This similarity between the sequence data and the established database sequence is shown in Figure 4.



BLAST search. These results indicate that both the method and the universal primers used in this study are conducive to this task. Due to poor amplification and transformation, the sequence of the *O. immunis* could not be amplified. More testing must be done to accomplish this. Future direction of this laboratory includes becoming the first lab to submit a formal sequence of the COI region in the species *O. compressus* to the BOLD Systems database. Ten sequences from each species will be collected in future experiments to be submitted to the BOLD database. In this way, the database will continue to grow and can be used in several fields of study, such as stream assessment.

As the method of study has been successful, the same technique will be applied to species of crayfish in the Schuylkill river basin of Pennsylvania in order to aid in bioassessment of stream health using macroinvertebrates. The procedure will look to find the sequence data for the invasive species *Orconectes rusticus*, the rusty crayfish, and a novel species from the *Cambarus acuminatus* complex called *Cambarus* [*Puncticambarus*] sp. C.<sup>12</sup>

## **Acknowledgements**

The authors would like to express their thanks and great appreciation to research advisor Dr. David Dunbar for his assistance and encouragement as well as his expert advice. Special thanks go to Dr. Kimberly Boyd for assistance in crayfish muscle dissection. The authors are very appreciative of chemical safety officer Cindy McGauley, and the Cabrini College Science Department. Without supportive family and friends, this research would not have been possible. Funds for this project were covered through an Environmental Protection Agency (EPA) Region III grant #9734890 entitled *Crabby Creek Stream Monitoring* given to Cabrini College.

## References

1. Herbert, P. D. N., Cywinska, A., Ball, S. L., & deWaard, J. R. (2003). Biological identification through DNA barcodes. *Proceedings of the Royal Society London B.*, 270, 313–321.
2. Castresana, J., Lubben, M., Saraste, M., & Higgins, D. G. (1994). Evolution of cytochrome oxidase, an enzyme older than atmospheric oxygen. *The EMBO Journal*, 13, 2516–2525.
3. Lynch, M., & Jarrell, P. E. (1993). A method for calibrating molecular clocks and its application to animal mitochondrial DNA. *Genetics*, 135, 1197–1208.
4. Ratnasingham, S., & Herbert, P. D. N. (2007). Bold: The barcode of life data system. ([www.barcodinglife.org](http://www.barcodinglife.org)). *Molecular Ecology Notes*, 7, 355–364.
5. Stoeckle, M. Y., & Herbert P. D. N. (2008). Barcode of life. *Scientific American*, \_\_, 82–87.
6. Meyer, C. P., & Pauley, G. (2005). DNA barcoding: error rates based on comprehensive sampling. *PLoS Biology*, 3, Retrieved May, 20, 2008, from <http://biology.plosjournals.org/perlserv/?request=getdocument&doi=10.1371/journal.pbio.0030422&ct=1>.
7. Rubinoff, D., Cameron, S., & Will, K. A. (2006). Genomic perspective on the shortcomings of mitochondrial DNA for “barcoding” identification. *Journal of Heredity*, 97, 581–584.
8. Smith, G. F., Roux, J. P., Tolley, K., & Conrad, F. (2005). Taxonomy and barcoding: Conflict or companion? *South African Journal of Science*, 102, 517–518.
9. Herbert, P. D. N., Penton, E. H., Burns, J. M., Janzen, D. H., & Hallwachs, W. (2004). Ten species in one: DNA barcoding reveals cryptic species in the neotropical skipper butterfly *Astraptes fulgerator*. *PNAS*. 101, 14812–14817.
10. Wong, E. H.-K., & Hanner, R. H. (2008). DNA barcoding detects market substitution in North American seafood. *Food Research International*, 41, 828–837.
11. Jackson, J. K. (2006). Long-term studies of freshwater macroinvertebrates: A review of frequency, duration, and ecological significance. *Freshwater Biology*, 3, 591–603.
12. Lieb, D. A. (2007). *Crayfish survey and discovery of a member of the *Cambarus acuminatus* complex (Decapoda: Cambaridae) at Valley Forge National Historical Park in southeastern Pennsylvania*. Technical Report NPS/NER/NRTR—2007/084. Philadelphia: National Park Service.

**An Analysis of the Effect of Pathogen-Associated Molecular Patterns (PAMPS) on Phagocytosis by Hyaline Amoebocyte Populations in the Earthworm *Eisenia hortensis*.**

Laura L. Goodfield and Sheryl L. Fuller-Espie

Faculty Advisor: Sheryl L. Fuller-Espie, Ph.D., DIC, Associate Professor of Biology

*Laura Goodfield completed two baccalaureate degrees at Cabrini College in May 2009, double majoring in Biology with a concentration in Biotechnology, and Spanish. Recruiting Laura to my research team in summer 2007 was one of the best decisions I have ever made! I was delighted and honored that she wanted to continue her research with me for two years. She investigated the cellular mechanisms of invertebrate immunity focusing primarily on cytokine-and PAMP-activated phagocytosis in earthworms. She received two student research grants from the Pennsylvania Academy of Science to fund her research projects. This year she presented her work at various venues including the Pennsylvania Academy of Science, the National Conference on Undergraduate Research, Pennsylvania Capitol Posters on the Hill event, and the Cabrini College Undergraduate Arts, Research and Scholarship Symposium, and published her findings in peer-reviewed journals. She co-authored "Conservation of cytokine-mediated responses in innate immunity: A flow cytometric study investigating the effects of human proinflammatory cytokines on phagocytosis in the earthworm *Eisenia hortensis*" which was published in *Invertebrate Survival Journal* (2008), and also published "A flow cytometric analysis of the effects of pathogen associated molecular patterns peptidoglycan and flagellin on phagocytosis in the earthworm *Eisenia hortensis* with enriched cell populations" in the *Proceedings of The National Conference on Undergraduate Research* (2009). This fall Laura will begin a doctorate degree in the Immunology and Infectious Disease program at the*



*Pennsylvania State University. Words cannot express my gratitude to Laura for her unwavering dedication to her research; those long hours in the lab really paid off in the long run and served to prepare her well for graduate school. Very few students exhibit the level of dedication that Laura possesses and I am very blessed to have had the opportunity to mentor her research for two exciting, productive, and memorable years.*

### **Abstract**

*Eisenia hortensis*, the earthworm also known as the European night crawler, is an invertebrate limited to an innate immune system. Although nonspecific, the innate immune system can generate a strong enough immune response to maintain the health of earthworms as they encounter microorganisms in their natural habitat in the soil. Their immune cells are derived from the coelomic cavity and can be categorized into three subpopulations: the hyaline amoebocytes (phagocytic activity), the granular amoebocytes (NK-like activity), and the eleocytes (lytic activity). This study focused on the effects of pathogen-associated molecular patterns (PAMPs), specifically peptidoglycan and flagellin, on the hyaline amoebocytes in *E. hortensis*. PAMPs are components of pathogens that make up molecular patterns identified by Toll-like receptors (TLRs) on immune cells. When a TLR identifies and binds to its PAMP, the receptor-ligand complex stimulates an innate immune response. Based on our previous studies with pretreatment with proinflammatory cytokines, we expected to see enhanced phagocytosis of the hyaline amoebocytes. To determine the level of immune response to flagellin and peptidoglycan, hyaline amoebocytes were first preincubated with different concentrations of PAMPs, and then exposed to *Escherichia coli* transformed with green

fluorescence protein (*E. coli*-GFP). Flow cytometric analysis of the immune cells was conducted to measure the level of specific phagocytosis of *E. coli*-GFP. Preliminary results ( $p \leq 0.05$ ) suggest that PAMPs do have an effect on the phagocytosis of *E. coli*-GFP compared to controls. Current studies are aimed at the development of procedure for enriching the hyaline amoebocyte subpopulation using Percoll gradient centrifugation. These studies will provide insight as to whether the coelomocyte subpopulation (granular amoebocytes and eleocytes) are having an indirect effect on phagocytosis by the hyaline amoebocytes by removing them from the PAMP-stimulated assay.

## **Introduction**

Many years ago in 1882, one of the first immunological discoveries was observed by Élie Metchnikoff (Beck & Habicht, 1996). He observed that the starfish, an invertebrate with a simple innate immune system, had immune cells that were fighting off a thorn, a potential threat to its survival, by attempting to engulf it. This observation was the scientific community's first exposure to phagocytosis. Since then, we have learned a great deal about the immune system and its many functions. However, there is still much more to learn. The immune system is an important factor to the survival of any organism, regardless of its complexity.

There are two types of immunity: innate immunity and adaptive immunity. Innate immunity is the immediate and primary response to foreign invaders and pathogens. This response is nonspecific, and is solely capable of maintaining the health of many organisms. Thus, the nonspecificity implies that these cells can and need to possess fixed receptors (Janeway & Medzhitov, 2002). This type of immunity is

incapable of remembering infections, and hence reacts the same way every time it encounters an invader. Innate immune responses include phagocytosis, encapsulation, natural killer-like activity, and agglutination, to name a few (Dhainaut & Scaps, 2001).

In contrast, adaptive immunity is a gradual and secondary response that is directed towards particular foreign invaders and pathogens, arming the immune system with a more powerful immune response and the memory to fight off future infections more efficiently. Adaptive immunity is based upon the function of T and B lymphocytes that have the ability to rearrange genetic material in order to bind specifically to certain antigens and pathogens to receptors (Janeway & Medzhitov, 2002). Adaptive immunity has evolved from innate immunity and, therefore, many similarities remain, alluding to their original function.

Although this study will focus on invertebrate immunity and more specifically innate invertebrate immunity, the scientific world has been able to make numerous connections between invertebrates and vertebrates. For example, Gerber, Cadet, Sheehan, Stegano, & Manton (2007) showed that invertebrate systems contain macrokines similar in function to cytokines found in vertebrates. A macrokine found in the snail *Biomphalaria glabrata* acts similarly to interleukin-1, a vertebrate cytokine responsible for cell proliferation stimulation (Beck, 1998). Another study (Fuller-Espie, Goodfield, Hill, Grant, & DeRogatis, 2008) supported conservation of receptors that bind to molecules that regulate innate immunity. Using human proinflammatory cytokines, an enhanced phagocytic immune response was stimulated in hyaline amoebocytes of the earthworm *Eisenia hortensis*.

For this study, coelomocytes from the earthworm *E. hortensis* were studied. Earthworms are used for immunological studies for several reasons: they are easy to care for, inexpensive to maintain, easy to work with in order to obtain the cells for culturing,

and most importantly, some of the immune responses have been shown to act similarly to their equivalents in vertebrates. In fact, the immune cells of earthworms have a comparable cellular structure and behavior to vertebrate leukocytes, especially involving processes such as phagocytosis (Vetvicka, Sima, Cooper, Bilej, & Roch, 1994).

Earthworm immune cells are derived from the coelomic cavity and can be categorized into three cellular subpopulations, each associated with different innate immune responses. For example, in *Dendrobaena veneta*, a species closely related to *E. hortensis*, the eleocytes (also known as chloragocytes) are small, very granular suspension cells that have lytic activity and make up about 30% of the coelomocyte population, though the portion may vary among species (Adamowicz & Wojtaszek, 2001). These coelomocytes exhibit a high level of autofluorescence, which makes it difficult to analyze these cells using fluorescence microscopy and flow cytometry. Eleocytes release eiseniapore, a lytic substance that is toxic to foreign cell types. Granular amoebocytes [also known as small coelomocytes (SC)] are small cells with significantly less granularity than the eleocytes; they exhibit natural killer-like activity, and make up about 28% of the coelomocyte population (Adamowicz & Wotjatazek, 2001). The granular amoebocytes recognize foreign invaders and pathogens and release enzymes such as lysenin, fetidin, lumbricin, and serine proteases in order to compromise the cell membrane of an invading cell, resulting in cell death (Cooper, Kauschke, & Cossarizza, 2002). Hyaline amoebocytes [also known as large coelomocytes (LC)] are large adherent cells with low granularity, and are capable of phagocytosis through microfilament extensions leading to the elimination of foreign invaders and pathogens via engulfment followed by degradation within the cell. In total, the hyaline amoebocytes make up approximately 42% of the cellular population (Adamowicz & Wotjatazek, 2001). These subpopulations can be viewed through microscopy (Figure

1A) and by flow cytometry based on forward scatter (size) and side scatter (granularity) (Figure 1B).

This study was aimed at the investigation of the affect of two PAMPs, flagellin and peptidoglycan, on phagocytosis. Using the hyaline amoebocytes as effector cells, the level of phagocytosis was measured with pretreatment of peptidoglycan and flagellin. Enhanced phagocytosis would suggest that hyaline amoebocytes have receptors, most likely PRRs similar or equivalent to TLRs, which contribute to the binding of the PAMP:receptor complex.

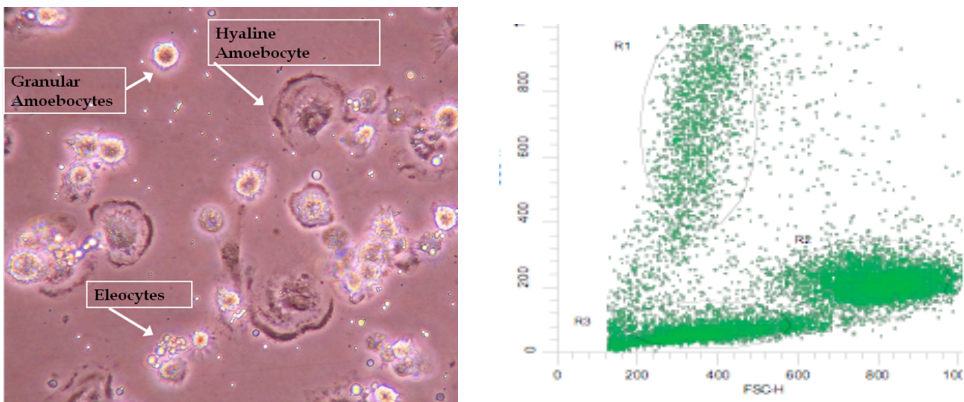


Figure 1. Typical display of coelomocytes from *Eisenia hortensis*. These cells were derived from the coelomic cavity through an extrusion process and then washed and resuspended in SDMEM. (A) represents coelomocytes viewed under a phase contrast inverted microscope. (B) is a dot plot (FSC vs. SSC) that illustrates the three subpopulations found in the coelomic cavity. Region 1 (R1) represents the eleocyte subpopulation, region 2 (R2) represents the hyaline amoebocytes (LC), and region 3 (R3) represents the granular amoebocytes (SC).

In vertebrates, the heterodimer TLR1/TLR2 has the ability to bind to peptidoglycan that is expressed as part of the cell wall of bacterial cells, especially in large quantities in gram positive bacteria. Other studies show that TLR2 is able to activate neutrophils, a type of lymphocyte capable of phagocytosing foreign materials (Kurt-Jones et al., 2002). The monomer TLR5 also binds to a PAMP, flagellin, found in motile bacteria (Francis, Wreesman, Yong, Reigstad, Krutzik, & Copper, 2007). Although earthworm TLRs have not yet been identified, the results of one group (Francis et al., 2007) suggest that earthworms may express many TLRs including TLR5, which may have bound to flagellin.

There are examples of phagocytosis using PRRs in invertebrates as well as the enhancement of phagocytosis using different stimulants. For example one group showed that the genetic sequence of *Caenorhabditis elegans* and *Caenorhabditis briggsae* encode TLRs (Zheng, Zhang, Lin, McIntosh & Malacrida, 2005). Other studies incubated earthworm cells with fluorescently labeled flagella (fl-flagellin) (Francis et al., 2007). Their results showed a positive shift in fluorescence of coelomocytes supporting the proposal that coelomocytes are able to bind to flagellin, most likely through a Toll-like receptor.

Based on the knowledge that hyaline amoebocytes have primarily phagocytic activity, this study focused on only the efficiency of this cell subpopulation and its immune responses. However, results showed enhancement and inhibition of phagocytosis. Thus, current investigations are aimed at the development of a purification procedure that will not compromise the phagocytic activity of the hyaline amoebocytes. In conjunction with this purification procedure, phagocytosis assays will continue to be carried out in order to determine the effect of the PAMPs flagellin and peptidoglycan on the efficiency of hyaline amoebocytes and their ability to phagocytose *E. coli*-GFP.

## Materials and Methods

### *Animal Husbandry*

*E. hortensis* colonies were purchased from Vermitechnology in Orange Lake, Florida and were maintained as detailed in Fuller-Espie et al. (2008) with modifications. Briefly, *E. hortensis* were kept in the dark at room temperature on moistened pine chips (LM Farm Animals ©) and shredded paper that have been autoclaved. Rice with Bananas Cereal (Gerber) was administered with water, and the bedding was changed twice weekly.

### *Cell Culture, Reagents, and PAMP Reconstitution*

All general reagents were purchased from Fisher-Scientific, and all cell culture reagents were purchased from Invitrogen unless otherwise mentioned. SDMEM contains Dulbeccos's Modified Eagle Medium supplemented with 10 % fetal calf serum, 100 mcg/mL ampicillin (Shelton Scientific), 10 mcg/mL kanamycin (Shelton Scientific), 10 mcg/mL tetracycline, 5 mcg/mL chloramphenicol (Fluka Biochemika), 1x penicillin/streptomycin/amphotericin B, 1x nonessential amino acids and 1x L-glutamine (Gibco). Flagellin (InvivoGen) was purified from *S. typhimurium* and peptidoglycan (InvivoGen) was purified from *Bacillus subtilis*. Each PAMP was reconstituted in sterile endotoxin-free water and frozen at  $-20^{\circ}\text{C}$  until use. PAMPs were used at varied concentrations, using PBS as the diluent, depending upon the assay (Tables 1 and 2).

*Bacterial Target Cells*

*Escherichia coli* HB101 was transformed with pGLO (BioRad) and subsequently plated onto tryptic soy agar supplemented with 100 mcg/mL ampicillin and 0.2% arabinose to selectively grow only those *E. coli* transformed with pGLO expressing the GFP (referred to as *E. coli*-GFP). After incubation with 4% paraformaldehyde for 1 hour at RT, *E. coli*-GFP were centrifuged at 3273xg and washed three times with phosphate buffer saline (PBS) (Invitrogen). *E. coli*-GFP were subsequently resuspended in PBS, enumerated on a hemocytometer, and stored at 4°C in the dark until use. The level of fluorescence was confirmed using a FACS Calibur flow cytometer and CellQuest Software (BD BioScience).

*Extrusion of Coelomocytes*

Earthworms with deep rich coloring and high activity, and lacking yellow appearance were placed on filter paper saturated in 1:10 dilution of 2.5 mcg/mL Fungizone (Fisher-Scientific) and povidone iodine (CVS Pharmacy) overnight. For all assays except the Percoll separation assay, coelomocytes are extruded according to Fuller-Espie et al. (2008). Briefly one earthworm was placed in a 100 mm Petri dish on ice containing 3 mL extrusion buffer (Extrusion buffer includes 71.2 mM NaCl, 5 % v/v ethanol, 50.4 mM guaiacol-glyceryl-ether, 5 mM EGTA, pH 7.3). For the Percoll separation assay, three to four earthworms were placed into a 100 mm Petri dish on ice containing 5 mL extrusion buffer. *E. hortensis* were removed, and the supernatant fraction was added to 1 mL Accumax. After incubation with Accumax at RT for 5 minutes, 5 mL PBS were added. Samples were centrifuged at 150xg for 5 minutes at



4°C. For all assays except Percoll separation assays, samples were resuspended in SDMEM; Percoll separation assay samples were resuspended in PBS. For all assays, samples were enumerated on a hemocytometer based on hyaline amoebocytes and given a quality score based upon the ratio of eleocytes to hyaline and granular amoebocytes.

#### *PAMP Phagocytosis Assays*

Coelomocytes were resuspended in SDMEM or PBS for PAMP assays or dose response assays, respectively, and the concentrations of coelomocyte samples were adjusted so that each well contained the same amount of hyaline amoebocytes as effector cells in 50 µL. PAMP Assay 1 used 45,000 effector cells/well, Assay 2 used 40,000 effector cells/well, and PAMP and dose response assays used 50,000 effector cells/well. Effector cells were pretreated with different concentrations of flagellin and peptidoglycan in triplicate. The plates were incubated overnight at 20°C with 5% CO<sub>2</sub>.

The next day control wells were pulsed with 5 µM cytochalasin B for PAMP assays and 5 µM for dose response assays. Following incubation at 30°C, for 30 minutes with 5% CO<sub>2</sub> in the dark, *E. coli*-GFP was added to each well with a multiplicity of infection (m.o.i.) of 1000 *E. coli*-GFP to 1 effector cell, totaling a volume of 150 µL. The plates were centrifuged briefly up to 150xg at 4°C, and each well was observed before incubation at 30°C at 5% CO<sub>2</sub>. PAMP Assay 1 was incubated for 1 hour with *E. coli*-GFP while the remaining assays were incubated for 2 hours. Directly following incubation, 0.02% Trypan Blue was added for quenching purposes (Mosiman, Patterson, Canterero, & Goolsby, 1997). Cells were harvested on ice and resuspended in FACS buffer for flow cytometric analysis.

*Six-Step, Discontinuous, Percoll Density Gradient*

Fifty mL conical test tubes were coated with 1% BSA and incubated overnight at RT on a rotator before making up the six-step gradients, consisting of 8 mL for each step for better separation. Gradients were stored overnight in the cold room until use. The next day, earthworms were extruded in batches of three earthworms to one 100 mm Petri dish containing 4 mL extrusion buffer. Extrusion was carried out as above, and samples were centrifuged at 150xg for 5 minutes at 4°C and enumerated on the hemocytometer before they were combined and added to the Percoll gradient. Gradients were centrifuged at 300xg for 12 minutes at 4°C. Fractions were separated according to banding patterns, washed with PBS twice at 150xg, and resuspended in 2 mL PBS. Samples were enumerated on the hemocytometer as well as analyzed on the flow cytometer. Two enriched batches with different proportions of hyaline amoebocytes to eleocytes (Batch 1 – 1:3, Batch 2 – 1:10) were pretreated overnight at 20°C with 1250 ng/mL peptidoglycan and flagellin in triplicate. The phagocytosis assay was carried out similarly to the dose response assays, using 50,000 effector cells and a m.o.i. of 1000 effector cells to 1 *E. coli*-GFP for 2 hours at 30°C.

*Flow Cytometric Analysis*

Flow cytometry was employed using a FACSCalibur flow cytometer (BD Biosciences) with an argon laser that excites GFP at 488 nm. GFP emits fluorescence at 530 nm and was measured using the FL-1 detector. Phagocytic assays were detected as detailed in Fuller-Espie et al. (2008) using the following instrument settings: forward light scatter (FSC): E-00 linear scale, side light scatter (SSC): 332 volts linear scale,

green fluorescence (FL-1): 312 volts log scale. *E. coli*-GFP alone was detected with the following altered settings FSC: E-03 log and SSC: log. Listmode data was acquired and analyzed using CellQuest software. All histograms and dot plots were created using WinList 5.0 (Verity Software House, Inc.) and were gated on cells matching the specifications (FSC vs. SSC) of the hyaline amoebocyte subpopulation. Percent specific phagocytosis was determined by subtracting the background (samples containing cytochalasin B) and comparing the samples in the absence and presence of flagellin or peptidoglycan.

### *Statistical Analysis*

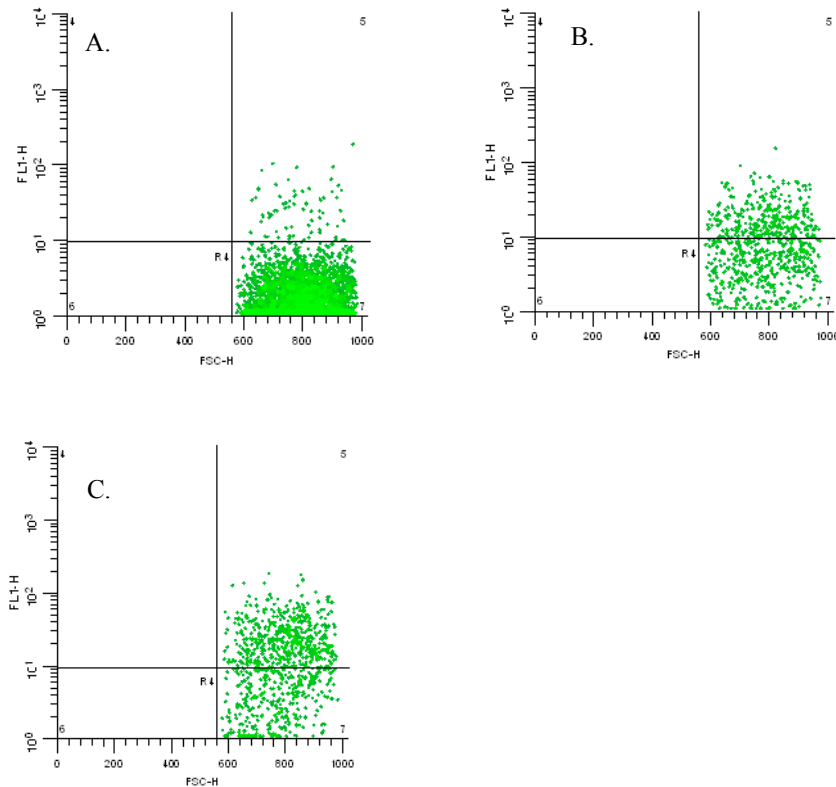
Credibility of the results was determined using the Student's *t* test as characterized by Microsoft Excel 2007. Only those results with  $p \leq 0.05$  were considered statistically significant. All graphs and charts were created using Microsoft Excel 2007.

## **Results**

### *PAMP and Dose Response Phagocytosis Assays*

A representative set of data are shown to illustrate enhanced phagocytosis when comparing the controls (Figure 2). In the first dot plot (Figure 2A), phagocytosis is inhibited by cytochalasin B, a microfilament inhibitor to determine the background of nonspecific binding. The second dot plot (Figure 2B) represents hyaline amoebocytes with *E. coli*-GFP alone, while the third dot plot (Figure 2C) represents hyaline amoebocytes with *E. coli*-GFP pretreated with a PAMP protein. A positive shift is

clearly seen when comparing each of the values, from negative control (Figure 2A) to effectors with *E. coli*-GFP (Figure 2B) to effectors with *E. coli*-GFP pretreated with PAMPs (Figure 2C), shifting upward towards higher fluorescence.



**Figure 2.** Enhanced Phagocytosis. This flow cytometric data represents a sample showing enhanced phagocytosis ( $p \leq 0.05$ ). (A) displays a two dimensional dot plot gated on the hyaline amoebocyte subpopulation measuring mean fluorescence of these cells from a sample containing effectors, *E. coli*-GFP, and cytochalasin B. (B) displays the same template from a sample containing effectors and *E. coli*-GFP as a means for comparison to the experimental value in (C), which was pretreated with a PAMP protein. Color contour from deep green to brighter green in each of the two dimensional dot plots shows the density of the cells.

These PAMP and dose response assays resulted in statistically significant responses for both peptidoglycan and flagellin and are summarized in Table 1 and Table 2, respectively. At 50 ng/mL peptidoglycan, 10% (2 out of 20) earthworms showed

enhanced phagocytosis. At 250 ng/mL 5% (1 out of 20) showed enhanced phagocytosis while 5% showed inhibition of phagocytosis. At 500 ng/mL peptidoglycan, 16.7% (1 out of 6) resulted in enhanced phagocytosis. At 50 ng/mL flagellin, a total of 10.75% (3 out of 28) earthworms exhibited enhancement of phagocytosis while 7.1% (2 out of 28) earthworms showed inhibition of phagocytosis. At 100 ng/mL flagellin, 16.67% (1 out of 6) earthworms exhibited enhanced phagocytosis. At 250 ng/mL flagellin, only 3.6% (1 out of 28) showed enhancement of phagocytosis while 17.9% (5 out of 28) showed inhibition of phagocytosis.

Table 1

*Peptidoglycan Summary*

	10 ng/mL	50 ng/mL	100 ng/mL	250 ng/mL	500 ng/mL	1250 ng/mL
PAMP 1			0/6		1/6 enhanced	
PAMP 2		0/6		1/6 inhibited		
PAMP 3		1/6 enhanced		0/6		
Dose Response 1	0/8	1/8 enhanced		1/8 enhanced		0/8
Total Response	0%	10% enhanced	0%	5% enhanced 5% inhibited	16.7% enhanced	0%

*Note.* This table illustrates a summary of all peptidoglycan concentrations tested in each particular assay and their results with regards to amount of earthworm responders as well as enhancement or inhibition. Only those earthworm responders that exemplified a statistically significant response ( $p \leq 0.05$ ) are shown.

Table 2

*Flagellin Summary*

	10 ng/mL	20 ng/mL	50 ng/mL	100 ng/mL	250 ng/mL	1250 ng/mL
PAMP 1		0/6		1/6 enhanced		
PAMP 2			0/6		1/6 inhibited	
PAMP 3			0/6		3/6 inhibited	
Dose Response 1	0/8		2/8 enhanced, 1/8 inhibited		1/8 inhibited	1/8 enhanced, 2/8 inhibited
Dose Response 2	0/8		1/8 enhanced, 1/8 inhibited		1/8 enhanced	3/8 enhanced
Total Response	0%	0%	10.7% enhanced 7.1% inhibited	16.7% enhanced	3.6% enhanced 17.9% inhibited	25% enhanced 12.5% inhibited

*Note.* This table illustrates a summary of all flagellin concentrations tested and their results with regards to amount of earthworm responders as well as enhancement or inhibition. Only those earthworm responders that exemplified a statistically significant response ( $p \leq 0.05$ ) are shown.

*Percoll Separation and Phagocytosis Assay*

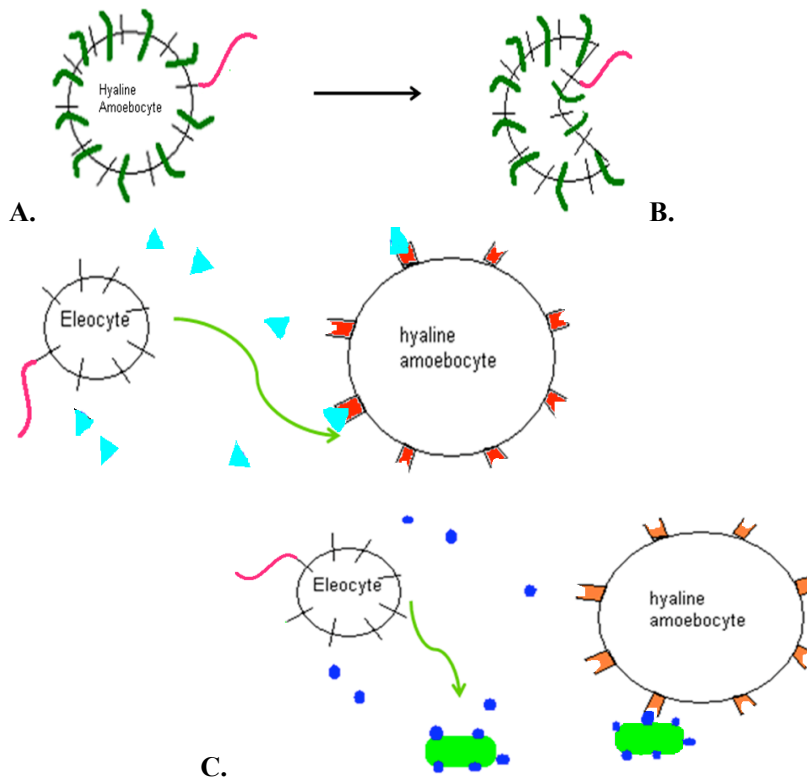
Two enriched batches resulted in different proportions of hyaline amoebocytes to eleocytes with Batch 1 having a 1:3 ratio and Batch 2 having a 1:10 ratio. Following data analysis with CellQuest, only one statistically significant batch (Batch 2) was found to have enhanced phagocytosis using 1250 ng/mL flagellin. There was no response to peptidoglycan.

## **Discussion**

These results suggest several different possible explanations of differing results. The hyaline amoebocyte may have bound to and internalized PAMPs during the preincubation period, resulting in a lower concentration of cell surface receptors (PRRs) available for binding to bacterial target cells (Figure 3A). Another explanation might be that in the presence of a high concentration of eleocytes, the eleocytes may have bound to the PAMPs, resulting in a release of macrokines that would in turn bind to hyaline amoebocyte macrokine receptors that caused an enhanced level of phagocytosis (Figure 3B). Yet another explanation might be that the eleocytes may have bound to the PAMPs, resulting in a release of opsonins that would in turn bind to bacterial targets, making them prime targets for hyaline amoebocyte phagocytosis (Figure 3C). A final explanation may be that earthworms are not an inbred population, due to their mode of sexual reproduction as hermaphrodites. They are highly polymorphic, resulting in the possibility of several different immune responses to a common pathogen.

## **Conclusion**

Preliminary results suggest that PAMPs may have an effect on phagocytosis, but this needs to be further studied. This study has also suggested that the presence of other PAMP-activated coelomocyte subpopulations (e.g. eleocytes) may have an indirect influence on the ability of hyaline amoebocytes to phagocytose target cells.



*Figure 3.* Possible mechanisms that occur with pre-incubation of PAMPs. (A) illustrates the concept of cell surface modulation, reducing the number of receptors found on the surface of the membrane that would aid in receptor mediated endocytosis. (B) illustrates the concept of macrokine release, following binding to a receptor, which would cause an upregulation of phagocytosis. (C) illustrates the concept of opsonization via eleocyte secretions, resulting in opsonization of bacteria for phagocytosis.

### Future Directions

Future directions include using a fluorescently tagged gram positive target cell like *Bacillus megaterium* for flow cytometric analysis. Another interesting experiment would be to investigate subsequent occurrences within the cell after phagocytosis of the target cell, for example conducting an oxidative burst assay to measure superoxide production during phagocytosis in response to PAMPs. Additionally, investigation of signal transduction pathways operating during PAMP:PRR binding is needed owing to



the lack of information available on what happens once the coelomocyte receives the signal. Perhaps instead of determining only the upregulation of the genes used as receptors, studies could investigate each individual step in which the cell undergoes activation, such as invertebrate homologs of the JAK/STAT or the NF-kappa B pathways.

### Acknowledgments

The authors wish to express their appreciation to the Pennsylvania Academy of Science and the Faculty Development Grant Committee of Cabrini College for grant support provided, and to colleague Katrina Hill.

### References

- Adamowicz, A., & Wojtaszek, J. (2001). Morphology and phagocytotic activity of coelomocytes in *Dendrobaena veneta* (Lumbricidae). *Zoologica Poloniae*, *46*, 91–104.
- Beck, G. (1998). Macrokines: Invertebrate-cytokine-like molecules? [Electronic Version]. *Frontiers in Bioscience*, *3*, d559–569.
- Beck, G. & Habicht, G. (1996). Immunity and the invertebrates. [Electronic Version]. *Scientific American*, 60–66.
- Cooper, E., Kauschke, E., & Cossarizza, A. (2002). Digging for innate immunity since Darwin and Metchnikoff. [Electronic version]. *Bio Essays*, *24*, 319–333.
- Janeway, C., & Medzhitov, R. (2002). Innate immune recognition. [Electronic Version]. *Annual Review of Immunology*, *20*, 197–216.
- Dhainaut, A., & Scaps, P. (2001). Immune defense and biological responses induced by toxics in Annelida. [Electronic version]. *Canadian Journal of Zoology*, *29*, 233–253.
- Francis, J., Wreesman, S., Yong, S., Reigstad, K., Krutzik, S., & Cooper, E. (2007). Analysis of the earthworm coelomocyte cell surface for the presence of Toll-like immune receptors. [Electronic version]. *European Journal for Soil Biology*, *42*, S92–S96.

- Fuller-Espie, S., Goodfield, L., Hill, K., Grant, K. & DeRogatis, N. (2008). Conservation of cytokine-mediated responses in innate immunity: A flow cytometric study investigating the effects of human proinflammatory cytokines on phagocytosis in the earthworm *Eisenia hortensis*. [Electronic version]. *Invertebrate Survival Journal*, 5, 124–134.
- Gerber, S., Cadet, P., Sheehan, M., Stegano, G., & Mantione K. (2007). Vertebrate interleukins originated in invertebrates? [Electronic version]. *Invertebrate Survival Journal*, 4, 95–100.
- Kurt-Jones, E., Mandell, L., Whitney, C., Padgett, A., Gosselin, K., Newburger, P., & Finber, R. (2002). Role of Toll-like receptor 2 (TLR2) in neutrophil activation: GM-CSF enhances TLR2 expression and TLR2-mediated interleukin 8 responses in neutrophils. [Electronic version]. *Blood Journal*, 100, 1860–1868.
- Mosiman, C., Patterson, B., Canterero, L., & Goolsby, C. (1997). Reducing cellular autofluorescence in flow cytometry: An in situ method. *Cytometry*, 30, 151–156.
- Vetvicka, V., Sima, P., Cooper, E., Bilej, M., Roch, P. (1994). *Immunology of Annelids*. Boca Raton, FL: CRC Press.
- Zheng, L., Zhang, L., Lin, H., McIntosh, M., & Malacrida, A. (2005). Toll-like receptors in invertebrate innate immunity. *Invertebrate Survival Journal*, 2, 105–113.

**Effects of Recombinant Human Cytokines Gamma Interferon, IL-10, and IL-12 on the Natural Killer-Like Response in *Eisenia hortensis* and its Method of Cytotoxicity**

Katrina M. Hill and Sheryl L. Fuller-Espie

Faculty Advisor: Sheryl L. Fuller-Espie, Ph.D., DIC, Associate Professor of Biology

*Doubling majoring in biology with a concentration in biotechnology, and mathematics, Katrina Hill completed her baccalaureate degrees at Cabrini College in May 2009. Rounding out her undergraduate curriculum, she was involved in an undergraduate research project in my lab that began September 2007 and concluded May 2009. During this time, Katrina participated in studies investigating the phagocytic and natural killer-like activities of invertebrates, cellular processes that are fundamental to the survival of animals with simple immune systems. She received a student research grant from the Pennsylvania Academy of Science in October 2008 to fund her research of innate immune responses in invertebrates. She has had numerous opportunities to present her research this year including the Pennsylvania Academy of Science; the National Conference on Undergraduate Research; the Pennsylvania Capitol Posters on the Hill event; and the Cabrini College Undergraduate Arts, Research and Scholarship Symposium. In addition, she coauthored "Conservation of cytokine-mediated responses in innate immunity: A flow cytometric study investigating the effects of human proinflammatory cytokines on phagocytosis in the earthworm *Eisenia hortensis*," which was published in *Invertebrate Survival Journal* (2008). She also published "Effects of recombinant human cytokines on the natural killer-like response in *Eisenia hortensis*: Cytotoxicity of invertebrate effectors revealed using a non-radioactive spectrophotometric assay" in the *Proceedings of the National Conference on Undergraduate Research* (2009). This fall Katrina will begin a Ph.D. program in Mathematical, Computational and Systems Biology at the University of*

*California- Irvine. It has been an honor mentoring Katrina over the past 2 years. I will miss her tremendously, but I am confident that she will continue to thrive in the challenging academic arena of graduate school and advance her scientific achievements to dizzying heights!*

### **Abstract**

The goal of this study was to determine the effect of recombinant human cytokines on natural killer-like activity in small coelomocytes from *Eisenia hortensis*, an earthworm also known as the European night crawler. Results from numerous immunological studies indicate that some species of invertebrates produce molecules with similar function to mammalian cytokines, and that mammalian cytokines initiate certain immune mechanisms such as phagocytosis, cytotoxicity, cell motility, and chemotaxis in invertebrates. For example, studies in the Fuller-Espie laboratory revealed enhanced phagocytosis in earthworm coelomocytes pretreated with four other proinflammatory cytokines, namely IL-1beta, IL-2, granulocyte-macrophage colony stimulating factor, and tumor necrosis factor-alpha. Here we report the effects of gamma interferon, IL-10, and IL-12 on cytotoxicity mediated by the small coelomocytes using the human erythroleukemic tumor cell line K562 as the target cell population. Cytotoxicity was measured using a nonradioactive cytotoxicity assay where cell membrane-compromised targets released lactate dehydrogenase into the supernatant fraction. This enzyme was quantified using a tetrazolium salt substrate that was converted into a red formazan product. Percent specific cytotoxicity for experimental and control samples was calculated taking maximum and spontaneous LDH-release values into account and comparing them to experimental values. Using the student's *t* test, only those samples

with  $p < 0.05$  were considered significant. After conducting seven assays in which 37 earthworms were tested, cytokine-treated earthworm cells exhibited a difference in NK-like killing compared to untreated control populations. Thus, it appears that recombinant human cytokines do influence cytotoxicity in the invertebrate *Eisenia hortensis*.

## Introduction

The immune system consists of an expansive array of molecules, cells, and tissues that interact together to form very complex responses to components that are recognized as foreign. Sometimes these invaders are foreign entities such as bacteria, fungi, or viruses; at other times, however, they can even be particles from the host's normal environment (allergens) or even components belonging to the host to which the body negatively reacts. These immune responses can be categorized as either innate or adaptive immunity. Innate immune reactions are nonspecific because they are not targeted against specific foreign components, but rather defend the body against a broad spectrum of entities.<sup>1</sup> Some of the processes used by innate immunity include phagocytosis, apoptosis, and natural killer-like (NK) activity.<sup>1</sup> These responses involve receptors that are always being expressed on the surface of cells and components that are always present in the serum (i.e., complement components); therefore, the responses can occur immediately after the organism is challenged and are often referred to as the "first line of defense."

Vertebrate NK cells, which are integral to innate immunity, help to eradicate foreign, infected, or tumorigenic cells via the polarized release of azurophilic granules from within the cytoplasm.<sup>2</sup> These granules usually contain perforin, granulysin, and granzyme, which create holes in the target's plasma membrane and the entry of

granzyme through the pore created on the target cell's surface by perforin triggers apoptosis, or programmed cell death.<sup>1,3</sup> The activity of NK cells is influenced by numerous cytokines including interleukin 10 (IL-10), IL-12, and gamma interferon ( $\gamma$ -IFN). IL-12, which is referred to as natural killer cell stimulatory factor, has been shown to stimulate NK cells to secrete  $\gamma$ -IFN and increase their cytolytic activity.<sup>4,5</sup>  $\gamma$ -IFN is responsible for stimulating macrophages, triggering antitumor defenses, and enhancing B cell and NK cell activation.<sup>6</sup> IL-10 is an anti-inflammatory cytokine that prevents the production of IL-12, along with TNF- $\alpha$  and IL- $\beta$ . TNF- $\alpha$  and IL- $\beta$  are cofactors that are involved in the initiation of  $\gamma$ -IFN production. IL-10 is produced by monocytes, B cells, and T cells.<sup>5</sup> Not only does IL-10 inhibit the activation of NK cells and thus  $\gamma$ -IFN production,  $\gamma$ -IFN has also been shown to inhibit IL-10 production in several cases.<sup>5</sup> IL-10, IL-12, and  $\gamma$ -IFN all trigger the Janus kinase (JAK-STAT) signal transduction pathway.<sup>6,7,8</sup>

Invertebrates, including earthworms, also have the ability to generate innate immune responses. These responses are vital to the survival of earthworms in their soil habitat. Innate immunity provides a very effective defense against contaminants and microbes that are abundant in the soil with which earthworms are constantly coming into direct contact.<sup>10,11</sup> As part of their humoral innate immunity, earthworms produce and secrete molecules including eiseniapore, fetidin, lysenin, coelomic cytolytic factor (CCF), and Lumbricin I that participate in the defense against microbes.<sup>12</sup> For example, in the earthworm *Eisenia fetida*, CCF binds to components on the outer surface of gram positive bacteria, gram negative bacteria, and yeast. This binding initiates the prophenoloxidase cascade that generates cytotoxic and antimicrobial molecules.<sup>12</sup> Because vertebrates possess both innate and adaptive immunity while invertebrates only have innate immune responses, a common conjecture is that cytokines involved in

adaptive immunity would only be found in vertebrates, but innate immunity cytokines and their homologues would be present in even the most unevolved animals.<sup>14</sup>

The earthworm coelomic cavity contains cells that participate in these innate immune responses. When analyzed via flow cytometry, these cells can be divided into three different populations based on size, granularity, and fluorescence.<sup>14, 15</sup> The small, less granular cells are referred to as granular amoebocytes or small coelomocytes. They are responsible for displaying NK-like activity.<sup>17</sup> The large, less granular cells are hyaline amoebocytes and, as stated earlier, are phagocytic.<sup>17</sup> The very granular cells are called eleocytes or chloragocytes and they play a role in earthworm nutrition, excretion, and the synthesis of molecules that are cytotoxic.<sup>18</sup> Eleocytes also exhibit some autofluorescence. Extensive study of the small coelomocytes has revealed that they possess mammalian cell surface molecules, including CD45RA, CD45RO, CD11a, CD-90, CD24, CDw49b, and CD54.<sup>2</sup> Because of the presence of these surface markers and the very effective NK-like ability of the small coelomocyte population, the theory that coelomocytes possess elements that are the evolutionary predecessors of leukocytes possesses some validity.<sup>2</sup> Furthermore, research has shown that, like mammalian NK cells, cell contact and the engagement of certain invertebrate effector receptors and target ligands might be important in ensuring adequate invertebrate cytotoxic activity.<sup>20</sup>

More recently, studies analyzing the effects of human recombinant cytokines on invertebrate innate immune responses are being performed. One such study<sup>14</sup> conducted in our lab measured the enhancement of phagocytosis of *E. coli* expressing green fluorescence protein (GFP) by *E. hortensis* coelomocytes after incubation with proinflammatory cytokines IL-1 $\beta$ , IL-2, TNF- $\alpha$ , and GM-CSF. Enhancement of phagocytosis was observed in samples pretreated with each of the cytokines and statistically significant response rates for each cytokine ranged from 10 to 30%. In

accordance with these interesting results, we speculated that the coelomocytes might possess receptors that are structurally similar to those on human phagocytes and, therefore, are able to bind the recombinant human cytokines and formulate an appropriate signal transduction cascade.<sup>14</sup>

Because of the accumulating data supporting conservation of innate immune responses, the associated effector molecules, and the receptors between invertebrates and vertebrates, additional study into the conservation of these innate mechanisms is becoming very popular. The ability of small coelomocytes to respond to recombinant human cytokines IL-10, IL-12, and  $\gamma$ -IFN was measured in this study using a nonradioactive LDH release assay coupled with spectrophotometric analysis.

## **Methods**

### *Animal Husbandry*

*E. hortensis*, the European night crawler (Vermitechnology Unlimited) were stored in plastic boxes containing wet, autocaved wood shavings and shredded paper. They were fed Gerber Rice with Bananas baby food cereal.

### *Extrusion*

The earthworm coelomocytes were first isolated by a process called extrusion. This involves the expulsion of the coelomic fluid, which contains the coelomocytes, from the coelomic cavity through the dorsal pores on the body of the earthworm upon agitation. Earthworms were individually placed overnight on filter paper saturated with a



1:10 povidone iodine-Fungizone solution containing 2.25 µg/ml Fungizone (Fisher Scientific) and 1% povidone iodine solution (CVS Pharmacy) to eliminate contamination by fungus and earthworm waste.

The following day, the earthworms were immersed in 3ml ice-cold, extrusion buffer (71.2 mM NaCl, 5 % v/v ethanol, 50.4 mM guaiacol-glyceryl-ether, 5 mM EGTA, pH 7.3). Then the supernatant fraction was incubated with 1 ml Accumax (Innovative Cell Technology) at room temperature for 5 minutes so that the protease, collagenase, and DNase activity of Accumax could break up the clumps of cells. After 5 minutes, 5 ml ice-cold 1x Dulbecco's phosphate buffered saline (PBS) (Gibco) were added in order to dilute the enzyme, and the solution was stored on ice. The sample was centrifuged at 149xg, 4°C, for 5 minutes to pellet the intact earthworm coelomocytes. The pellet was resuspended in 1 ml Dulbecco's modified eagle medium (DMEM) unless otherwise stated, and the concentration was determined using a hemocytometer and an inverted phase contrast microscope.

#### *Target Cell Culture*

Cells from the human erythroleukemic tumor cell line K562 were expanded in DMEM in a tissue culture flask at 37°C and 5% CO<sub>2</sub>. The intact cells were then pelleted via centrifugation at 335xg for 5 minutes at 4°C. The pellet was resuspended in 1 ml DMEM before the concentration was determined using a hemocytometer and an inverted phase contrast microscope.

*Natural Killer-Like Activity Assay*

The natural killer-like activity assay was performed in order to determine the effect that recombinant human cytokines  $\gamma$ -interferon ( $\gamma$ -IFN), interleukin 10 (IL-10), and interleukin 12 (IL-12) have on earthworm coelomocytes regarding their cytotoxic properties. K562 cells were used as targets for killing. Several different types of samples were involved in this assay: a control for spontaneous killing of coelomocytes (coelomocytes and media), a control for natural fluorescence of media (media alone), a control for spontaneous killing of K562 target cells (K562 cells and media), a control for normal coelomocyte cytotoxicity levels (coelomocytes, K562 cells, and media), a control for maximum killing of targets (K562 cells, lysis solution, media), a volume corrected control to account for any dilution of the fluorescence due to the addition of the lysis solution to the target maximum lysis control (media and lysis solution), a control for fluorescence from K562 cells incubated with the cytokine, and the experimental samples (coelomocytes, targets, and cytokine). Lysis solution, tetrazolium salt, Stop Solution, LDH positive control, Assay Buffer, and cytotoxicity assay protocol were provided in the Cytotox 96 Non-Radioactive Cytotoxicity Assay kit (Promega).

Earthworm coelomocytes were harvested and resuspended in 1 ml HyClone DME/High Modified DMEM without phenol red, which was supplemented with 5% fetal calf serum and 100  $\mu\text{g/ml}$  ampicillin (Shelton Scientific), 10  $\mu\text{g/ml}$  kanamycin (Shelton Scientific), 10  $\mu\text{g/ml}$  tetracycline, 5  $\mu\text{g/ml}$  chloramphenicol (Fluka Biochemika), 1x penicillin/streptomycin/amphotericin B, 1x nonessential amino acids, and 1x L-glutamine (Gibco) to make super (SDMEM).

The cells were counted, and their concentration was adjusted to  $1 \times 10^6$  cells/ml. Then 50  $\mu\text{l}$  of the coelomocytes, the appropriate amount of low phenol red SDMEM,

and 50 µl cytokine (40 ng/ml) were added to the relevant wells of a 96-well plate. Then the plate was incubated at 20°C, 5% CO<sub>2</sub> overnight. The target cells were harvested, washed, and resuspended in low phenol red SDMEM, and their concentration was adjusted to 2x10<sup>5</sup> cells/ml before 50 µl (10,000 cells) were added to the appropriate wells. The plate was centrifuged at 149xg for 1 min to encourage contact between the coelomocytes and the targets and incubated for 3.25 hr at 30°C, 5% CO<sub>2</sub>. Lysis solution (20 µl) was added to the maximum target lysis control, and the volume corrected control, and the plate was incubated for another 45 min. The plate was then centrifuged at 250xg for 4 min at 4°C. A solution containing the chromogenic tetrazolium salt substrate was prepared by combining 12 ml Assay Buffer and 1 bottle of the substrate provided in the kit. After 50 µl of each supernatant fraction was placed into a new well of a 96-well flat bottom plate, 50 µl of the substrate solution was added. The plate was incubated for 30 min at room temperature in the dark so that the lactate dehydrogenase could convert the substrate into a red formazan product that absorbs at 490 nm. Then 50 µl Stop Solution were added to all wells. Any bubbles in the samples were popped with a needle and the samples were analyzed by an Ultramark plate reader (BioRad) at 490 nm. Percent specific cytotoxicity for the untreated and cytokine-treated samples containing coelomocytes and targets was determined using the absorbance values measured for the samples and the percent cytotoxicity equation:

% cytotoxicity =

$$\frac{\text{Experimental Sample} - \text{Spontaneous Coelomocyte Lysis} - \text{Spontaneous Target Lysis}}{\text{Maximum Target Lysis} - \text{Spontaneous Target Lysis}} \times 100 \quad (1)$$

Maximum Target Lysis – Spontaneous Target Lysis

The calculated percent cytotoxicity for the untreated sample was then compared to the percent cytotoxicity for the cytokine treated sample using the Student's *t* Test defined by Microsoft Excel 2007, and only samples with *p* values less than or equal to 0.05 were considered significant.

For some of the assays, the plates containing the samples were stored at  $-80^{\circ}\text{C}$  for several hours before continuing with the protocol. This freezing was expected to have no effect on the activity of the lactate dehydrogenase because Shain, Boesel, Klipper, and Lancaster found that total LDH activity was not altered after human plasma was stored at  $-90^{\circ}\text{C}$  for 4 to 6 weeks.<sup>20</sup>

## Results

The NK-like activity experiment was performed by first treating earthworm coelomocytes with IL-10, IL-12, or  $\gamma$ -IFN overnight. Then the target cells were added to the sample and incubated for 4 hr. The cells were spun down in order to prepare a cell-free supernatant fraction to which a chromogenic substrate was added. LDH released by killed cells into the supernatant fraction converted the salt into a red formazan product that absorbs at 490 nm. The absorbance was measured using an Ultramark plate reader and the percent cytotoxicity was calculated. Experimental samples with percent cytotoxicity values statistically different from those of the background cytotoxicity controls (determined using the Student's *t* Test and requiring that  $p \leq 0.05$ ) were identified.

Overall, 4 earthworms out of the total 37 tested with the cytokines, or 10.8%, responded with enhanced cytotoxicity to IL-10 pretreatment (Table 1). Twice as many (8 out of 37 or 21.6%) earthworms responded with inhibited cytotoxicity after the IL-10

pretreatment (Table 1). Regarding IL-12 pretreatment, 9 out of 37 (24.3%) earthworms responded with enhanced cytotoxicity while 5 out of 37 (13.5%) responded with reduced cytotoxicity (Table 1). After treatment with  $\gamma$ -IFN, 7 out 37 (18.9%) exhibited enhanced cytotoxicity and 4 out of 37 (10.8%) displayed reduced cytotoxicity (Table 1).

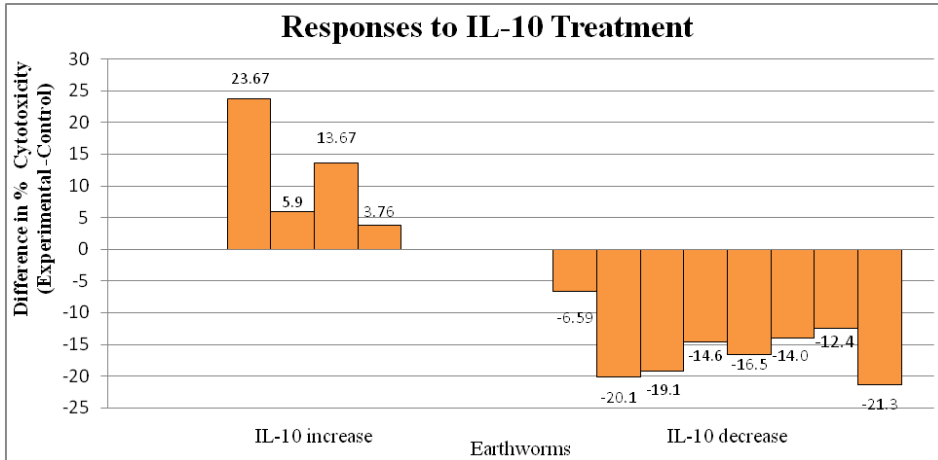
Table 1

*Percent Responders to Cytokine Treatment*

<b>Response</b>	<b>Responders / Total Tested</b>	<b>Percentage of Responders (%)</b>
Enhancement by IL-10	4/37	10.8
Inhibition by IL-10	8/37	21.6
Enhancement by IL-12	9/37	24.3
Inhibition by IL-12	5/37	13.5
Enhancement by $\gamma$ -IFN	7/37	18.9
Inhibition by $\gamma$ -IFN	4/37	10.8

*Note.* Coelomocytes were pretreated with IL-10, IL-12, or  $\gamma$ -IFN and were incubated with targets. Samples with significantly affected percent specific cytotoxicity values—determined using the Student’s *t* Test ( $p \leq 0.05$ )—were counted and the percent of significant responders out of the total number of earthworms tested was determined.

Earthworms tested in the cytotoxicity assays were referred to by the assay number in which they were used and the number given to them in the assay (typically 1–8). The earthworms that responded to IL-10 pretreatment with enhanced cytotoxicity were earthworms 3.3 (Assay 3, Earthworm 3), 3.7, 4.8, and 5.3 with enhancements of 23.67%, 5.9%, 13.67%, and 3.76%, respectively (Figure 1). Cytotoxicity by Earthworms 3.6, 4.2, 4.4, 4.7, 6.4, 6.6, 6.7, and 6.8 decreased by 6.59%, 20.1%, 19.1%, 14.6%, 16.5%, 14.0%, 12.4%, and 21.3%, respectively, after treatment with IL-10 (Figure 1).



*Figure 1.* Effect of IL-10 treatment on percent cytotoxicity of coelomocytes. Extruded earthworm coelomocytes pretreated with IL-10 were incubated with K562 targets and percent cytotoxicity was determined using a nonradioactive LDH cytotoxicity assay. The percent cytotoxicity measured for the background cytotoxicity control was subtracted from the percent cytotoxicity calculated for experimental samples that were deemed statistically significant using the Student's *t* Test ( $p \leq 0.05$ ). This difference represents the magnitude of the response by the coelomocytes to the treatment with IL-10. Earthworms that exhibited enhanced cytotoxicity after treatment of the coelomocytes with IL-10 were grouped together in the graph (IL-10 increase) and those that exhibited reduced cytotoxicity after treatment with IL-10 were grouped together (IL-10 decrease).

Earthworms 2.6, 3.1, 3.4, 3.5, 3.7, 3.8, 5.1, 5.2, and 5.5 exhibited enhancements of 25.16%, 20.77%, 19.67%, 27.67%, 7.16%, 11.5%, 21.91%, 1.2%, and 16.43%, respectively, in response to IL-12 treatment (Figure 2). Decreases in percent cytotoxicity of 4.44%, 5.45%, 14.29%, 9.57%, and 31.38% were calculated for Earthworms 2.1, 3.6, 4.1, 4.4, and 6.4 (Figure 2).

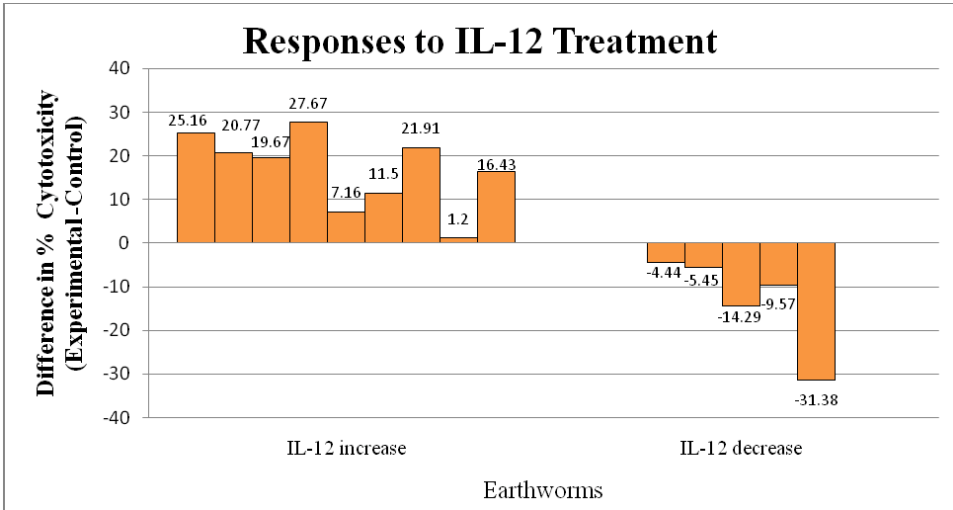
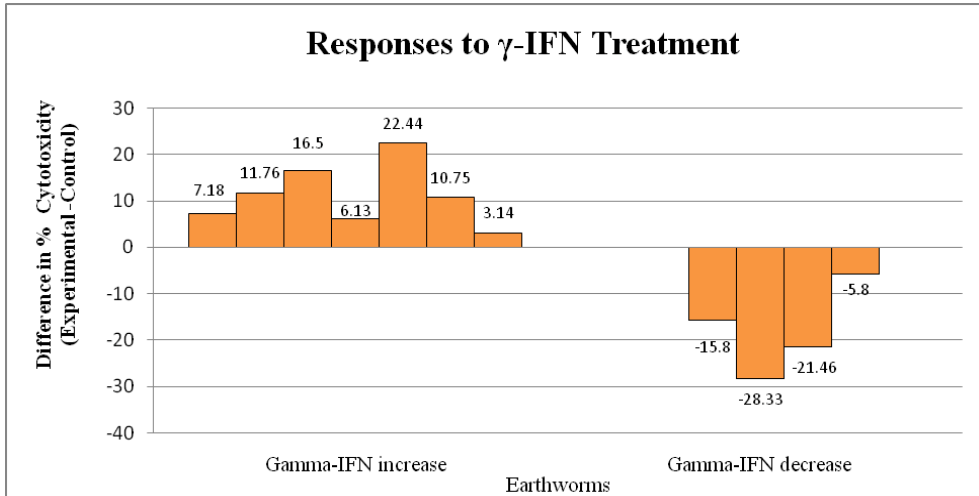


Figure 2. Effect of IL-12 treatment on percent cytotoxicity of coelomocytes. Extruded earthworm coelomocytes pretreated with IL-12 were incubated with K562 targets and percent cytotoxicity was determined using a nonradioactive LDH cytotoxicity assay. The percent cytotoxicity measured for the background cytotoxicity control was subtracted from the percent cytotoxicity calculated for experimental samples that were deemed statistically significant using the Student’s *t* Test ( $p \leq 0.05$ ). This difference represents the magnitude of the response by the coelomocytes to the treatment with IL-12. Earthworms that exhibited enhanced cytotoxicity after treatment of the coelomocytes with IL-12 were grouped together in the graph (IL-12 increase) and those that exhibited reduced cytotoxicity after treatment with IL-12 were grouped together (IL-12 decrease).

Percent cytotoxicity of Earthworms 2.6, 3.7, 5.1, 5.2, 5.3, 5.5, and 5.7 was enhanced by 7.18%, 11.76%, 16.5%, 6.13%, 22.44%, 10.75%, and 3.14%, respectively, following treatment with  $\gamma$ -IFN (Figure 3).  $\gamma$ -IFN treatment reduced percent cytotoxicity of Earthworms 3.6, 4.7, 4.8, and 6.3 by 15.8%, 28.33%, 21.46%, and 5.8%, respectively (Figure 3).



*Figure 3.* Effect of treatment on percent cytotoxicity  $\gamma$ -IFN of coelomocytes. Extruded earthworm coelomocytes pretreated with  $\gamma$ -IFN were incubated with K562 targets and percent cytotoxicity was determined using a nonradioactive LDH cytotoxicity assay. The percent cytotoxicity measured for the background cytotoxicity control was subtracted from the percent cytotoxicity calculated for experimental samples that were deemed statistically significant using the Student's *t* Test ( $p \leq 0.05$ ). This difference represents the magnitude of the response by the coelomocytes to the treatment with  $\gamma$ -IFN. Earthworms that exhibited enhanced cytotoxicity after treatment of the coelomocytes with  $\gamma$ -IFN were grouped together in the graph ( $\gamma$ -IFN increase) and those that exhibited reduced cytotoxicity after treatment with  $\gamma$ -IFN were grouped together ( $\gamma$ -IFN decrease).

## Conclusion

Numerous responders were identified in the NK-like activity assay, but the same cytokines induced opposite responses. These data suggest that IL-10 caused inhibitory effects in more samples than it caused enhancement because twice as many earthworms responded with inhibited cytotoxicity. In humans, IL-10 is known to inhibit the activity of NK cells.<sup>4</sup> Similarly, almost 1 of every 4 earthworms tested responded with enhanced cytotoxicity to IL-12, but 13.5% showed inhibition. Enhancement occurred nearly twice as often in comparison to inhibition. Because human NK cells are stimulated by IL-12 to become more cytotoxic,<sup>4</sup> the results from this study could be a preliminary indication that many earthworms respond to IL-12 in a similar fashion as humans.



In addition, nearly twice as many earthworms (18.9% vs. 10.8%) responded with enhanced cytotoxicity to  $\gamma$ -IFN over inhibited cytotoxicity so again, this very preliminary evidence suggests that many earthworms respond as humans do to  $\gamma$ -IFN since  $\gamma$ -IFN is associated with the cytotoxic activity of human NK cells.<sup>20</sup> Therefore, it is tempting to speculate that earthworms respond to cytokines through similar signal transduction pathways compared to those used in vertebrate cells. However, further experimentation is needed to reveal the exact mechanism by which human cytokines are stimulating immune responses in earthworms.

The earthworms that were used in these experiments are polymorphic because they are not derived from an inbred population. This could mean that the earthworms being tested have polymorphic receptors for the cytokines and that some receptors bind to the cytokine, inducing enhanced cytotoxicity, while allelic variants of the same receptor, possibly with a slightly different structure, bind to the cytokine, but instead mediate an inhibitory effect on cytotoxic activity. Therefore, it is possible that the apparent opposing responses to the cytokines were caused by the polymorphic heterogeneity of the earthworms.

Stronger inhibitory and stimulatory responses might also have been detected if the coelomocyte population being used was more pure and contained only small coelomocytes. Only minimal enrichment of the small coelomocyte population was attempted in these studies because efficient and effective purification techniques have not yet been developed for earthworm coelomocytes. During the coelomocyte harvesting process, efforts were made to remove as many chloragocytes as possible by making them adhere to the top of the pipette during pipetting and mixing steps. Also, earthworms were selected initially to be extruded based on the color of their bodies—deep red earthworms compared to those with yellower coloring typically extrude fewer

chloragocytes. In addition, after harvest and enumeration of the coelomocytes, each batch of coelomocytes from each earthworm was scored based on the number of chloragocytes present; batches with high numbers of chloragocytes were given lower scores and only the highest scoring batches were used in the assays. Despite all of these measures, chloragocytes, sometimes great in number, were present in the samples. Chloragocytes possess chloragosomes containing a wide variety of molecules that are released into the solution surrounding the cell.<sup>14</sup> These molecules might have altered how the small coelomocytes were responding to the cytokines.

In future studies purification of individual coelomocyte populations could be attempted via flow cytometric cell sorting, or by combining a Percoll gradient with an adherence purification step to separate out chloragocytes and large coelomocytes respectively. These types of purification assays will be dependent on the development of monoclonal antibodies specific for cell surface molecules of earthworm coelomocytes unique to the different cell subpopulations. To date, these reagents do not exist.

### **Acknowledgments**

The author would like to thank the following individuals for their assistance and support: Laura Goodfield, a colleague; her family; the undergraduate research grant committee of the Pennsylvania Academy of Science for funding K. Hill; and the Cabrini College Faculty Development Research Grant committee for funding S. Fuller-Espie.

## References

1. Orange, J. S., & Ballas, Z. K. (2006). Natural killer cells in human health and disease. *Clinical Immunology*, 118, 1–10.
2. Cossarizza, A., Cooper, E. L., Suzuki, M. M., Salvioli, S., Capri, M., Gri, G. et al. (1996). Earthworm leukocytes that are not phagocytic and cross-react with several human epitopes can kill human tumor cell lines. *Experimental Cell Research*, 224, 174–182.
3. Elmore, S. (2007). Apoptosis: A review of programmed cell death. *Toxicology Pathology*, 35(4), 495–516.
4. Scharton-Kersten, T., Afonso, L. C. C., Wysocka, M., Trinchieri, G., & Scott, P. (1995). IL-12 is required for natural killer cell activation and subsequent T helper 1 cell development in experimental leishmaniasis. *Journal of Immunology* 154, 5320–5330.
5. D'Andrea, A., Aste-Amezaga, M., Valiante, N. M., Xiaojing, M., Kubin, M., & Trinchieri, G. (1993). Interleukin 10 (IL-10) inhibits human lymphocyte interferon  $\gamma$ -production by suppressing natural killer cell stimulatory factor/IL-12 synthesis in accessory cells. *Journal of Experimental Medicine*, 178, 1041–1048.
6. Meager, A. (2006). *The Interferons*. Weinheim: Wiley.
7. Watford, W. T., Moriguchi, M., Morinobu, A., O'Shea, J. J. (2003). The biology of IL-12: Coordinating innate and adaptive immune responses. *Cytokine & Growth Factor Reviews*, 14, 361–368.
8. Donnelly, R. P., Dickensheets, H., & Finbloom, D. S. (1999). The interleukin-10 signal transduction pathway and regulation of gene expression in mononuclear phagocytes. *Journal of Interferon & Cytokine Research*, 19(6), 563–573.
9. Salzet, M., Tasiemski, A., & Cooper, E. (2006) Innate Immunity in Lophotrochozoans: The Annelids. *Current Pharmaceutical Design*, 12(24), 3043–3050.
10. Cooper, E. (2006). Role of TOLL-like receptors in adjuvant-augmented immune therapies by T. Seya. *Evidence-based Complementary and Alternative Medicine*, 3(1), 133–137.
11. Engelmann, P., Cooper, E. L., & Nemeth, P. (2005). Review anticipating innate immunity without a TOLL. *Molecular Immunology*, 42, 931–42.
12. Bilej, M., De Baetselier, P. Van Dijck, E., Stijlemans, B., Colige, A., & Beschin, A. (2001). Distinct carbohydrate recognition domains of an invertebrate defense molecule recognize gram-negative and gram-positive bacteria. *Journal of Biological Chemistry*, 276, 45840–45847.
13. Kaiser, P., Rothwell, L., Avery, S., & Balu, S. (2003). Evolution of the interleukins. *Developmental and Comparative Immunology*, 28, 375–394.

14. Fuller-Espie, S. L., Goodfield, L., Hill, K., Grant, K., & DeRogatis, N. (2008). Conservation of cytokine-mediated responses in innate immunity: A flow cytometric study investigating the effects of human proinflammatory cytokines on phagocytosis in the earthworm *Eisenia hortensis*. *Invertebrate Survival Journal*, 5, 124–134.
15. Patel, M., Francis, J., Cooper, E. L., & Fuller-Espie, S. L. (2007). Development of a flow cytometric, nonradioactive cytotoxicity assay in *Eisenia fetida*: An in vitro system designed to analyze immunosuppression of natural killer-like coelomocytes in response to 7, 12 dimethylbenz[a]anthracene (DMBA). *European Journal of Soil Biology*, 43S1, S97–103.
16. Komiyama, K., Yoshimura, M., Okaue, M., Iwase, T., Cooper, E.L., Okumura, K., & Moro, I. (1998). Perforin in earthworm coelomocytes. *Developmental and Comparative Immunology*, 22, 133–134.
17. Engelmann, P., Molnar, L., Palinkas, L., Cooper, E.L., & Nemeth, P. (2004). Earthworm leukocyte populations specifically harbor lysosomal enzymes that may respond to bacterial challenge. *Cell Tissue Research*, 316, 391–401.
18. Suzuki, M. M., & Cooper, E. L. (1995). Killing of intrafamilial leukocytes by earthworm effector cells. *Immunology Letters*, 44, 45–49.
19. Shain, S. A., Boesel, R. W., Klipper, R. W., & Lancaster, C. M. (1983). Creatine kinase and lactate dehydrogenase: Stability of isoenzymes and their activity in stored human plasma and prostatic tissue extracts and effect of sample dilution. *Clinical Chemistry*, 29(5), 832–835.
20. Schroder, K., Hertzog, P. J., Ravasi, T., & Hume, D. A. (2004). Interferon- $\gamma$ : An overview of signals, mechanisms, and functions. *Journal of Leukocyte Biology*, 75, 163–189.

## Computational Studies of Novel Nano Substructures

Erin McCole

Brittany McIntyre

Faculty Advisor: Joseph M. Smith, Associate Professor of Chemistry

*Erin T. McCole is a 2009 graduate from Cabrini College with a B.S. in chemistry. Erin earned the chemistry departmental award for academic excellence and served the college through a number of activities such as a choir member and as an officer of the Cabrini science club. As part of her chemistry program requirement, she participated in a 2008 summer chemistry internship at Cephalon, Inc., where she carried out experiments involving generation and analysis of combinatorial libraries. She also chose to study fluorescent tagging in combinatorial libraries for her senior seminar capstone project. Erin has since been accepted into the Ph.D. program in chemistry at Temple University.*

*As an undergraduate, Erin approached me with an interest in undergraduate research in the area of computational studies in the area of nanotechnology. We carried out a systematic study of small molecules that mimicked substructures in multiwalled carbon nanotubes. In particular, HOMO and LUMO energies were determined and compared as a function of pyramidalization and torsion of orbitals comprising a p bond. Erin presented her results, along with Brittany McIntyre, at the 2009 Cabrini Undergraduate Research Symposium*

## Abstract

The recent discovery of multiwalled carbon nanotubes (MWCNs) has sparked a great deal of interest and research. The structure of MWCNs is such that all carbon atoms are slightly pyramidalized. Consequently, *s* character is engendered into what would normally be unhybridized *p* orbitals in a planar system. The degree of pyramidalization should correlate with the diameter of the nanotube. Further, there appears to be two types of relationships between adjacent carbons; those where  $\pi$  interactions result from pyramidalized orbitals that are coplanar and those where  $\pi$  interactions occur between orbitals where the torsion angle is other than zero. Quantum mechanical calculations were carried out in order to study both types of  $\pi$  interactions using simple molecules designed to mimic isolated segments of nanotubes of differing diameters. In particular, values for HOMO and LUMO energies were calculated and compared as well as values for other characteristics such as carbon–carbon double bond stretching frequencies and bond lengths.<sup>1</sup>

## Background

Carbon nanotubes were first discovered in 1991 by Sumio Iijima. He accidentally discovered these structures while researching the graphite electrode surfaces that are utilized in an electric arc discharge.<sup>2</sup> Prior to this discovery, a new form of elemental carbon known as C<sub>60</sub>, or the buckyball had been discovered in 1985 by several scientists from the University of Sussex. Nanotubes are made up of graphite-like elemental carbon. The majority of the rings that make up a nanotube are C<sub>6</sub> rings, but there are enough C<sub>5</sub> rings that the cylinder structure is able to form. Carbon nanotubes

are either multiwalled (MWNT), which were the first type found in 1991, or single-walled (SWNT), which were discovered in 1993. These are illustrated in Figure 1. Also, they are either closed at one end or both ends, and since the ends of a carbon nanotube undergo more strain than the rest of the structure, they are more chemically reactive.<sup>3</sup>

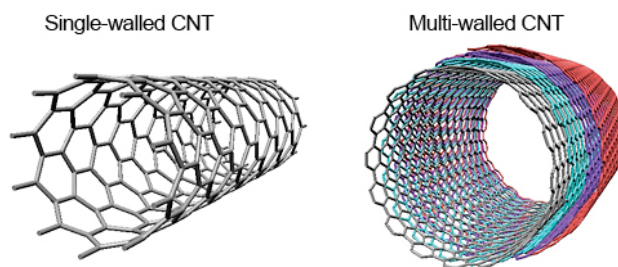


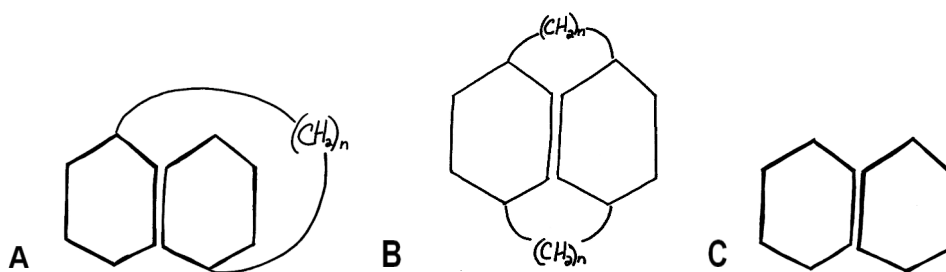
Figure 1. Single-walled carbon nanotube versus multiwalled carbon nanotube.<sup>4</sup>

Multiwalled and single-walled carbon nanotubes are of great scientific and commercial interest because of their exceptional structural, chemical, electrical, and thermal properties. Due to such properties, they have a wide range of applications. Their structural properties include having high strength and being one of the stiffest materials ever made, but also having elasticity. This property makes carbon nanotubes suitable for the aerospace and fiber industries. The electronic properties include their conductance and unique semiconducting capabilities, which make this material perfect for nanoelectronics and semiconductors. Also, carbon nanotubes are capable of hydrogen adsorption (storage) and, thus, can be used in hydrogen-based fuel cells. They even have electronic sensitivity in different chemical environments, which could make them valuable as novel environmental sensors. For these reasons, it is expected that the supply and demand for carbon nanotubes will continue to expand rapidly.<sup>5</sup>

To meet such supply and demand, there is a need for multiple means of synthesizing carbon nanotubes. Some of the processes for synthesizing both SWNT and

MWNT include arc evaporation, laser vaporization, and chemical vapor deposition, and solid-state metathesis reactions. Multiwalled nanotubes can be synthesized from decomposition reactions, and by heating a polymer resin as well.<sup>6</sup>

To study further some of the properties of carbon nanotubes, we decided to try to mimic segments of a nanotube using various molecules. Each molecule has a common scaffold consisting of two, six-membered rings attached to one another through a carbon-carbon double bond. These rings are pulled out of planarity using tethers of varying length and in varying positions. In this manner, our molecules imitate the rings that make up a carbon nanotube, which are all pulled out of planarity. The molecules we studied can be classified into two different groups. We labeled the first group Co-Planar because the three molecules that make up this group all have two different methylene side chains that act as tethers inflicting strain on the scaffold. Part A of Figure 2 represents the basic structure of this group. We labeled the second group Torsion because the three molecules that make up this group all have a methylene tether of varying lengths that stretches from the end of one six-membered ring in the scaffold across to the end of the other, six-member ring, pulling both rings out of planarity. Part B of Figure 2 shows the basic structure of this group. We also studied a reference molecule consisting of only the basic scaffold, common throughout all of our molecules, which we labeled Planar and can be seen in part C of Figure 2.



*Figure 2.* Structures of compounds mimicking segments of carbon nanotubes. (A) Co-Planar group. (B) Torsion group. (C) Planar Reference Compound. Methylene bridge tethers were varied in length for A and B to vary the degree of  $\pi$  interaction.



The reasoning for changing the lengths of the methylene bridge tethers for each compound is to study the  $\pi$  interactions between the  $p$  orbitals of the carbon-carbon double bond. Figure 3 is a picture of the predicted hybridized orbitals resulting from being pulled out of planarity.

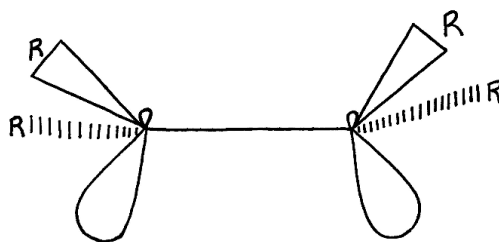


Figure 3. Diagram of hybridized  $\pi$  orbitals.

The molecular structure of the Planar Reference compound R is seen in Figure 4. Figure 5 lists the three compounds classified as Co-Planar. Compound A was termed 1C Co-Planar because there is one carbon in each of the side chains; Compound B has two carbons in the side chains, so we called it 2C Co-Planar; and lastly, Compound C has three carbons in each of the methylene chains, so it was labeled 3C Co-Planar. Figure 6 lists the three compounds classified as Torsion. Compound D was named 2C Torsion because there are two carbons in the methylene bridge; Compound E has three carbons in the chain, so it was called 3C Torsion; and finally, Compound F has four carbons in the methylene tether, so we termed it 4C Torsion.

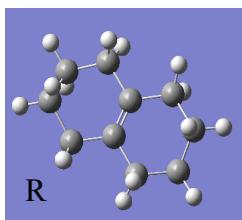


Figure 4. Planar compound. This molecule was used as a reference for the other six compounds.<sup>8</sup>

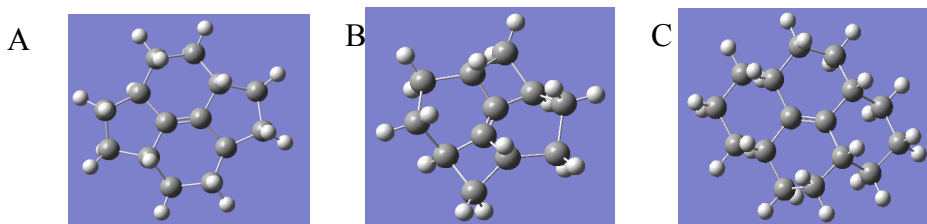


Figure 5. Co-planar compounds. (A) 1C Co-Planar. (B) 2C Co-Planar. (C) 3C Coplanar.<sup>8</sup>

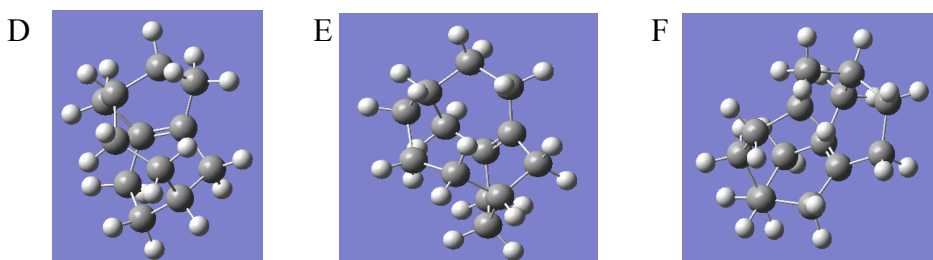


Figure 6. Torsion compounds. (D) 2C Torsion. (E) 3C Torsion. (F) 4C Torsion.<sup>8</sup>

## Methods

To conduct our molecular modeling research, we used a computational computer program package known as Gaussian 03 with GaussView 4.<sup>7,8</sup> Calculations were carried out using the Gaussian 03 software package, restricted Hartree Fock (RHF) level of theory, and a 3-21 G basis set. We performed RHF based calculations since they are the simplest default and therefore take less time. The results of these calculations can be considered our baseline to which future calculations will be compared. For each of the seven molecules that we studied, we wanted to determine the optimal structure of the molecule and calculate the energy of it, as well as the HOMO and LUMO energies, the carbon-carbon double bond distance, and the frequency of that double bond. The planar

molecule (Figure 4) was used as a control against which we could measure our resulting data.

For each of the seven molecules, the same basic procedure was followed. First the molecule was constructed using the builders toolbar, and when completed, it was named appropriately (refer to Figures 4, 5, and 6) and saved as a GIF file. Next, the Calculate button was clicked and from the list that appeared, Gaussian Calculation Setup was chosen. When the Gaussian Calculation Setup window appeared, the calculation type was changed to Optimization and the Submit button was clicked. Then another window appeared requesting that the model be saved again. The molecule was once again saved as a GIF file; however, the number two was added to the original name it was saved under. Upon completion of these calculations, the file containing the summary of the results was opened and from that data, the energy of the molecule (E(RHF)) was recorded. When multiple E(RHF) values were calculated, the one resulting from the most cycles performed was recorded. A picture of the optimized geometry was obtained by opening the checkpoint file (.chk) for the compound. The carbon-carbon double bond distance was determined by clicking on those two carbons of the checkpoint molecule and recording the bond distance value that appeared. Next, the HOMO and LUMO energies were extracted from the results by clicking Edit and from the list choosing the Molecular Orbitals symbol. The energy of the LUMO was found by choosing LUMO under Add Type in the Visualize tab of the window and then clicking update. Once the screen was updated with these changes, the actual LUMO was clicked on and the value was recorded, and a picture of the LUMO was obtained. The value for the HOMO was found and recorded, and a picture of it was obtained in the same manner.

The second type of calculation performed was for vibrational frequency. Similar to the procedure above, the Gaussian Calculation Setup window was opened, however, the calculation type chosen was Frequency, and the box that said Compute Projected Frequency was checked. Once again, after clicking Submit, the molecule needs to be saved, so the number three was added to the original name of the compound, and it was saved as a GIF file. When the calculations were completed, the Results button was clicked and from the list, Vibrations was chosen. In the window that appeared the stretching frequencies of the molecule were demonstrated by clicking on the first frequency in the list and then clicking on the Start Animation button. The vibrational frequency corresponding to the carbon–carbon double bond was determined by scrolling down the list until the desired vibrational animation was seen animated by the molecule, then that frequency was recorded. However, the Gaussian frequency values are always skewed from the actual frequency values of the physical molecule, and therefore need to be adjusted by a scaling factor.

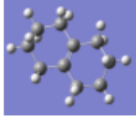
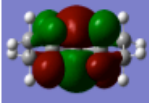

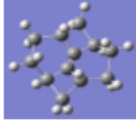
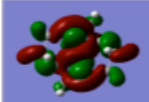
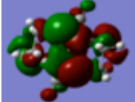
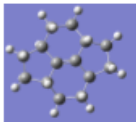
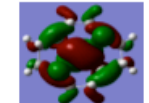
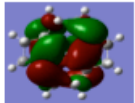

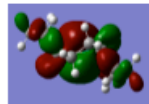
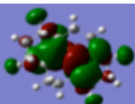
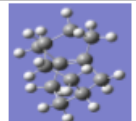
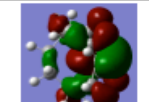
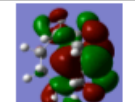
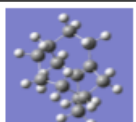
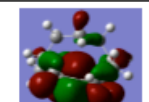
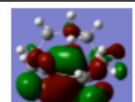
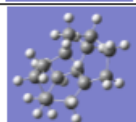
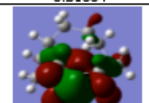
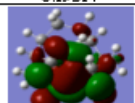
The scaling factor was calculated using the data calculated for the planar reference molecule. Since the vibrational frequency for a carbon–carbon double bond is normally at  $1620\text{ cm}^{-1}$ , the value of the scaling factor is equal to  $1620\text{ cm}^{-1}$  divided by the vibrational frequency of the planar compound as calculated by Gaussian. After the numerical value was determined, the scaling factor was used to normalize the vibrational frequencies of interest for each of the six models being studied. Thus, the vibrational frequency of the carbon–carbon double bond for each of the other six molecules was multiplied by the calculated scaling factor, resulting in a normalized frequency that was then recorded.

After all of the necessary calculations for all seven of the compounds were completed and the desired information was recorded, the data was compiled in a chart.

The chart was reviewed and the trends observed among the Torsions compounds were noted and compared to the trends observed among the Co-Planar compounds.

Table 1

*Results of Quantum Mechanical Calculations Performed on the Molecules Mimicking Isolated Segments of Carbon Nanotubes*

Molecule	Energy of Molecule (Hartree)	Optimization	C=C Bond Distance (Å)	HOMO Energy (Hartree)	LUMO Energy (Hartree)	C=C Vibrational Frequency (cm <sup>-1</sup> )
<b>Planar</b>	-385.848772367		1.3218	 -0.3189	 0.20187	1620
<b>1C Co-Planar</b>	-460.68294535		1.05187	 -0.25426	 0.16554	3133.246058
<b>2C Co-Planar</b>	-538.783304247		1.29775	 -0.28029	 0.17741	1712.535956
<b>3C Co-Planar</b>	-616.464803996		1.36375	 -0.31161	 0.18874	1598.17131
<b>2C Torsion</b>	-462.275127314		1.32297	 -0.30693	 0.18427	1622.54257
<b>3C Torsion</b>	-500.747094945		1.32128	 -0.31067	 0.19514	1607.865391
<b>4C Torsion</b>	-539.577141891		1.32062	 -0.31153	 0.19419	1612.984547

## Results

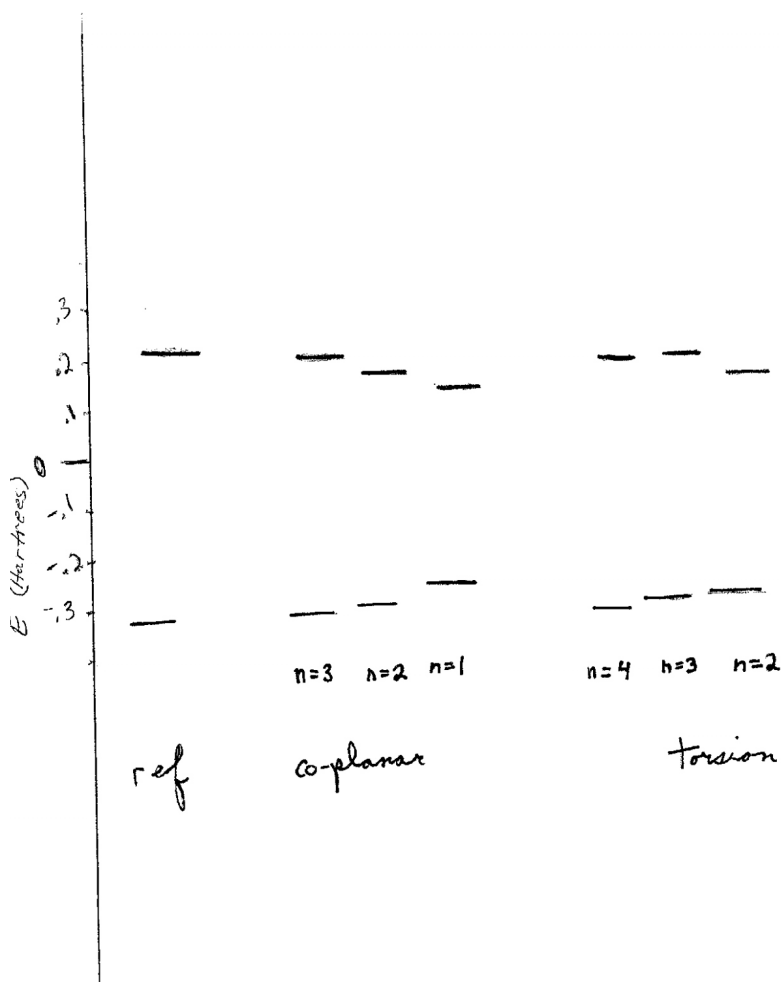


Figure 7. HOMO and LUMO energy diagram.

## Discussion

As indicated in Table 1, the HOMO energies increased and LUMO energies decreased as the number of carbons in the methylene bridge tethers decreased. Figure 7 is a visual representation of the HOMO's and LUMO's for all of our molecules and the gap in between each molecule's HOMO and LUMO. This trend in HOMO and LUMO energy values was expected because as the number of carbons in the chains decreases

consistent with this and indicates a decrease in  $\pi$  overlap. Also, this observed decrease in the HOMO/LUMO gap as the strain from the tethers increases, imitates what is known of carbon nanotubes, for as the HOMO/LUMO gap decreases, it is easier for electrons to move from the HOMO to the LUMO, which in turns means that it is easier for that substance to conduct electricity. Carbon nanotubes are known for conducting electricity, and their conductivity increases as their diameter decreases, so our data is consistent with this information.

The energy of the molecule also increased as tethers were shortened. This also supports what we predicted, for as the strain energies increase the molecules are more unstable. Therefore, their lowest energy confirmations should have a higher energy value.

In general, these structures showed good trends in the values for tether length, carbon-carbon double bond length, and vibrational frequency and they showed good correlation between each category. The only structure that did not fit into the trends was the 3C Torsion compound, which was perhaps due to some computational error.

However, the majority of the trends were opposite to what was expected. This is most likely due to structural perturbations on the olefinic carbon-carbon single bond, because this single bond also influences the length and vibrational frequency of the double bond.

Yet, the increase in vibrational frequency as the strain increases does seem to make some physical sense. One would expect the  $\pi$  bond to get lower in frequency as the orbitals are pulled farther apart, so in that sense the trend seems backwards. However, the energy of the molecule is directly proportional to the frequency according to the equation  $E = hv$ , where  $E$  is the energy,  $h$  is Planck's constant, and  $v$  is the frequency.

As the strain increases on our models, they increase in energy because they are less

stable. The energy is directly proportional to the frequency; therefore, it makes sense that, as strain increases, frequency increases as well.

In summary, for this research on mimicking segments of carbon nanotubes, two things are happening to the molecules imitating these segments. As they are pulled out of planarity by the tethers we have added, we are changing the nature of the  $p$  orbitals and changing the degree of overlap of these orbitals. By straining the molecules, “ $s$ ” character is engendered in to the  $p$  orbitals transforming them from unhybridized orbitals to hybridized orbitals. As the orbitals associated with the carbon–carbon double bond are pulled farther apart, they are less able to interact, which in turn destabilized the bonding orbital (HOMO) and stabilizes the antibonding orbital (LUMO). Therefore, the HOMO energy increases and the LUMO energy decreases (i.e., the HOMO/LUMO gap decreases). The HOMO and LUMO play a large part in determining the properties and chemical reactivity of a molecule; therefore, the more strain that is put on the molecule, the more those properties will change.

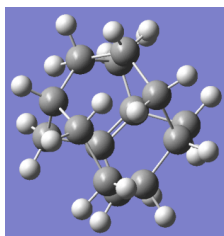
### **Future Directions**

Possible future directions that could be taken include performing Unrestricted Hartree Fock (UHF) based calculations on the seven molecules that we constructed. While RHF based calculations are a useful starting point for our research, they are not as accurate as calculations that are more sophisticated like UHF based ones. Unrestricted Hartree Fock calculations will probably take longer to complete with Gaussian since they are much more complex, however, they will probably yield results that are more accurate for HOMO and LUMO energies, and carbon–carbon double bond length and



stretching frequency. These results can then be compared to the results we have thus far obtained from RHF calculations.

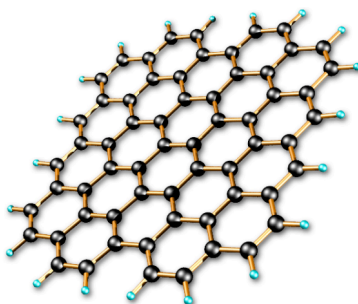
In the future different molecules could be constructed that might better mimic isolated segments of carbon nanotubes. In particular, we could perform calculations on molecules with two tethers stretching across from the end of one ring to the end of the second ring, as seen in Figure 8. The length of these methylene bridge tethers could be varied as they were in the Torsion and Co-Planar compounds we researched. Perhaps this new group of molecules would show a decrease in the interference of the  $\sigma$  bonds, thereby allowing us to focus more on the  $\pi$  orbital interaction. In other words, these new models may perturb the  $\sigma$  bonds less than our current models do, which could increase the accuracy of some of the data values resulting from our quantum mechanical calculations.



*Figure 8:* Future model to mimic an isolated segment of a carbon nanotube. This molecule is a modified version of the Torsion and Co-Planar Models with two methylene bridge tethers stretching from one end of the first, six-membered ring to the end of the second, six-membered ring. Two carbons make up each of the tether chains in this particular molecule; however, the chain can be expanded to three or more carbons and could also be shortened to one carbon.<sup>8</sup>

A more novel form of elemental carbon has been discovered since the birth of the carbon nanotube, one that is gaining much popularity among the scientific community. This form of carbon is known as graphene. Graphene is a thin, single layer of carbon atoms bound tightly together in a honeycomb structure that was first isolated in 2004. In reality, graphene has been around long before this discovery, for graphite is

thought to be made up of layers of it, and carbon nanotubes and buckyballs are thought of as rolls of the material. Widespread interest in graphene was sparked by the material's surprising characteristics, such as its highly desirable structural, mechanical, and electronic properties. It has been found to be a very stiff and very strong material that is faster at conducting electrons at room temperature than anything else. Therefore, many scientists predict that graphene could be potentially be used for circuit components of various electronic technologies. Applications of graphene as well as methods of synthesizing it are currently being researched by scientists in both industry and academia.<sup>9</sup> Figure 9 is a picture of graphene.



*Figure 9.* Graphene structure.<sup>10</sup>

Therefore, while there is still much to be studied on the properties of carbon nanotubes, another option for future research could involve studying the properties of graphene using molecular modeling. Then the results of the graphene Gaussian calculations can be compared to the results from the nanotube research.

### **Acknowledgments**

I would like to thank my mentor Dr. Smith for his insight and guidance throughout this process. I also want to thank Brittany McIntyre for working alongside of me to conduct this research.

## References

1. Smith, J. (2009, April). *Computational studies of novel nano substructures*. Radnor, PA: Cabrini College.
2. Ajayan, P. M. (2002). Carbon nanotubes. In H. S. Nalwa (Ed.), *Handbook of nanostructured materials and nanotechnology* (pp. 329–357). San Diego: Academic Press.
3. Klabunde, K. J., & Mulukutla, R. S. (2001). Chemical and catalytical aspects of nanocrystals. In K. J. Klabunde (Ed.), *Nanoscale Materials in Chemistry* (p. 243). New York: John Wiley and Sons.
4. University of Waterloo School of Pharmacy. About Dr. Marianna Foldvari. ([www.pharmacy.uwaterloo.ca/.../about/index.html](http://www.pharmacy.uwaterloo.ca/.../about/index.html)[accessed May 6, 2009]).
5. Hyung, H., Fortner, J. D., Hughes, J. B., & Kim, J-H. (2007). Natural organic matter stabilizes carbon nanotubes in the aqueous phase. *Environmental Science Technology*, *41*, 179–184.
6. O’Loughlin, J. L., Kiang, C.-H., Wallace, C. H., Reynolds, T. K., Rao, L., & Kaner, R. B. (2001). Rapid synthesis of carbon nanotubes by solid-state metathesis reactions. *Journal of Physical Chemistry*, *105*, 1921–1924.
7. Gaussian 03, version 7.1, 1994–2005. (2005). Wallingford, CT: Gaussian, Inc. (ISBN: 0-9727187-2-9).
8. GaussView 4, version 4.1, 1997–2007. (2007). Wallingford, CT: Gaussian, Inc. (ISBN: 978-0-9727187-5-2).
9. Jacoby, M. (2009, March). Graphene: Carbon as thin as can be. *Chemical and Engineering News*, \_\_\_\_, pp. 14–20.
10. Science @ Berkeley lab. ([www.lbl.gov/.../Archive/sabl/2007/Nov/gap.html](http://www.lbl.gov/.../Archive/sabl/2007/Nov/gap.html)[May 11, 2009]).

## **Modeling Tetra Coordinate Cu(I) Binding Proteins**

Robert E. De Vasto, Jeffery D. Evanseck, and Melinda A. Harrison

Faculty Advisor: Dr. Melinda Harrison

*Robert completed his undergraduate research on a project that blends mathematical principles and equations with chemistry bonds and small atomic molecules. Robert graduated from Cabrini College in May 2009 with a major in mathematics and a minor in chemistry. Robert began the project in December of 2008 and was selected for a competitive Undergraduate Research Program at Duquesne University for the Summer of 2009 in Pittsburgh, Pennsylvania, to continue his studies on this project. Robert will work full-time for 10 weeks on the project and will be mentored by Dr. Jeffery Evanseck a leader in the computational field. His studies will be incorporated into a peer-reviewed journal article. The project was originally started by then graduate student Melinda Harrison in her dissertation work at Duquesne University. Dr. Harrison worked with Dr. Evanseck on the project and performed the calculation of the linear and trigonal planar coordination of the Cu(I) ion to the cysteinyl sulfur ligands. Robert has taken his part of the project and truly excelled with his research efforts. He enjoyed the project so much that he was recommended and accepted into the summer research program mentioned above. I am grateful to Robert for all his hard work and am eager to watch him blossom into a full-time researcher. His family and I are very proud of him. This project has peaked Robert's interest into now applying to graduate schools for fall 2010 to design small molecules for drug applications.*

## Abstract

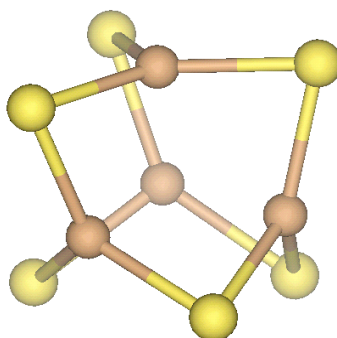
Copper(I) proteins are found on the cell membrane and also inside the cell. These proteins play a role in redox activity; help to transfer Cu(I) throughout the cell and also to rid the body of toxic material. A great of research has been done on the *in vivo* and *in vitro* protein interactions, but not much research has been completed on the structure of the Cu(I) binding site. Cu(I) binds to the cysteines within a protein structure and can form different coordination to the sulfurs in the cysteines. For example: Cu(I) can bind to two cysteines and take a linear configuration; Cu(I) can bind to three cysteines and take a trigonal planar coordination and lastly two proteins can join through a Cu(I) ion through a tetrahedral coordination with 4 sulfur ligands. The overall purpose of the project is to understand how Cu binds to multiple Sulfurs in protein structures. This research will involve computer modeling in which various lengths, angles, dihedrals and vibrational frequencies of Cu bounded by four cysteinyl sulfurs will be determined. The mathematical program, Gaussian, was used for all calculations. For each specific model, B3LYP was used and combined with a basis set which determines the accuracy of the results. Model 1 will be using B3LYP/3-21g; Model 2 will be using B3LYP/6-31g(d) and Model 3 will use B3LYP/6-31+G(d,p). Further calculations will be run using various equations similar to Model 3. From the results determined via computations, the best Cu-cysteinyl sulfur model will be determined.

## Introduction

Copper is an essential trace element, which enters the body through diet. Any large amount of Copper contained in the body will become very toxic for the body.<sup>1</sup> The main organ, which processes copper, is the liver, which serves to transport the copper to various locations. The trace element copper is used as a cofactor for redox and hydrolytic proteins. Copper is utilized in electron transfer processes because of its ability to cycle between the oxidation states of Cu(I) and Cu(II).<sup>2</sup> Copper ions can also be toxic to both eukaryotic and prokaryotic cells because of their ability to aid in the formation of oxygen radicals, which can cause oxidative damage to proteins, nucleic acids, and lipids.<sup>1</sup> Therefore, the regulation of the intercellular levels and location of copper ions is crucial to cellular homeostasis.<sup>3</sup> Copper has been known to bind with sulfur, oxygen, and nitrogen within protein structures.

Over the past few decades, there have been numerous solution structures solved of Cu(I) proteins, including the Cu(I) chaperones: Atx1 (yeast), CopZ (bacteria), Cox17 (yeast) and Ccc2a (yeast), the ATPases in *B. subtilis* (Ctr1), the Second Metal Binding Domain of the Menkes Protein (ATP7A) and also of the redox proteins of Cu(I) SOD.<sup>4-9</sup> The Cu(I) is bound to the cysteinyl sulfur ligands in these proteins in either a linear, trigonal planar or tetrahedral like arrangement. The Cu(I) chaperones contain a single metal binding motif consisting of Met-x-Cys-x-x-Cys and the metal is proposed to be bound to the sulfur ligands in the cysteines in a linear coordination.<sup>7, 10, 11</sup> It has also been proposed that Cu(I) in the same motif may induce dimerization of two chaperone-like proteins and in this case the metal would be coordinated to the sulfur ligands in either a tetrahedral coordination or a distorted trigonal planar fashion rather than linearly. This type of arrangement has been proposed by O'Halloran et al. for Atx1 and by Rosenzweig et al. for the human chaperone, Hah1.<sup>4, 12</sup>

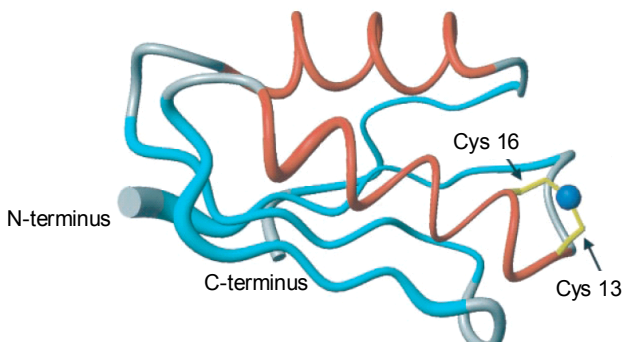
In the case of the metallotheoin's (MT's), which can have several cysteine repeats within their protein sequence, the Cu(I) coordination is more complex. A trigonal planar coordination has been proposed with several cysteinyl sulfurs ligands and several Cu(I) ions involved, therefore making the structure more "cage-like" with bridging Cu(I)-S clusters. One of the first examples of this type of polycopper cluster formation was shown by Ian Dance et al. and his crystal structure (See Figure 1 below).<sup>13</sup> Other groups have used his crystal structure as the model for their protein's polycluster site. Mac1 and Ace1 are two Cu(I) responsive transcriptional regulators that contain multiple cysteine binding sites and are both proposed to bind several Cu(I) ions.<sup>6</sup> Researchers believe the Cu(I) are bound to the sulfurs in a bridging manner and most of the Cu(I) ions are arranged in a trigonal planar coordination.<sup>6, 14</sup>



*Figure 1.* Ace1/Mac1 metal binding site postulated structure. The polycopper cluster proposed by Winge et al. which is believed to be similar in Mac1 and Ace1. Copper binds to the regulatory proteins within their cysteine-rich motif, copper's are shown in red and sulfurs in yellow, note each Cu(I) within the structure is bridging.<sup>6</sup>

A linear Cu(I) coordination due to the presence of only two cysteines and no methionines nearby could also be possible and has been proposed. The yeast Cox17, a Cu(I) binding protein, has been proposed to bind Cu(I) with its lone -Cys-x-x-Cys- metal binding motif.<sup>8</sup> Also the yeast copper transporter Ccc2a has been shown to bind Cu(I) in

the same way. Its NMR structure is available in the Cu(I) loaded form and is shown in Figure 2.



*Figure 2:* Cu(I) loaded Ccc2a solution structure. The backbone atoms for the solution structure are shown as a tube proportional to the backbone of the protein. The cysteine 13 and 16 side chains, and the Cu(I) atom are shown.<sup>9</sup>

DFT has provided reasonable results on small Cu(I)-S clusters.<sup>15-17</sup> Cu(I) molecules have been studied by a few groups, however, none have provided much detail concerning Cu(I)-S ligand coordination and its application to proteins.

The structure of proteins can be seen through normal structural methods such as NMR and crystallography. In the case of Cu(I) proteins, the usual methods such as NMR and crystallography will be unable to formally give a good interpretation of the Cu(I) placement because NMR and crystallography cannot be used for Cu(I) detection. NMR calculations typically benefit most from very accurate geometries and larger basis sets. In addition, the accuracy for NMR is much lower compared to the methods of the Gaussian program. This is why Gaussian is being used, because it is an alternative approach to being able to understand the structure of Cu(I) proteins.

The overall purpose of the project is to understand how Cu binds to multiple Sulfur atoms in protein structures. This research will involve computer modeling in which various lengths, angles, dihedrals and vibration frequencies of Cu bounded by



four cysteinyl sulfurs will be determined. The mathematical program, Gaussian, was used for all calculations. For each specific model, the method B3LYP was used and combined with a basis set that determines the accuracy of the results. Model 1 will be using B3LYP/3-21g level of theory; Model 2 will be using B3LYP/6-31g(*d*) level of theory, and Model 3 will use B3LYP/6-31+G(*d,p*) level of theory. From the results determined via computations, the best Cu-cysteinyl sulfur model will be determined.

### **Experimental Method**

For this research, a certain basis set is required to deem a precise depiction of what the protein structure would appear as within the cell. The program used, Gaussian, is a complex mathematical program that uses specific calculations to predict energies, molecular structures, and vibration frequencies of molecular systems and their molecular properties by using specific basis sets and equations.<sup>18</sup> Gaussian is an advanced program that is being utilized to help the scientific community progress deeper within molecular systems for better understandings of how they work. Gaussian offers a wide variation of DFT, Density Functional Theory models. DFT methods are used because they include effects of electron correlation, which is where electrons in molecular system react of other electrons motion and try to avoid each other.<sup>18</sup> DFT not only takes into account for the electron density, but also the instantaneous interactions of pairs of electrons with opposite spin. Most DFT formulations are divided into components, which are calculated individually such as kinetic energy, electron-nuclear interaction, Coulomb repulsion, and an exchange-correlation term for remainder electron-electron interaction.<sup>18</sup> The DFT used will be B3LYP. DFT is a breakdown of understanding where each part of the model chemistry comes from. The LYP part of the model chemistry comes from the

correlation functional of Lee, Yang, and Parr, which includes both local and nonlocal terms.<sup>19</sup> They are methods that when read by the program can compute the specific equations needed. All the methods need to be combined with the specific keyword for the desired exchange function. Therefore, for the B3LYP model the B stands for Becke's exchange functional and the LYP correlation functional. The last part of the model chemistry would be the "3," which stands for the parameter function.<sup>19</sup> Each method used needs a basis set. A basis set is the mathematical description of the orbital's that are used in combination to approximate the total electronic wave function.<sup>18</sup> Standard basis sets will use linear combinations of Gaussian functions to create the orbitals. The basis sets can be improved by increasing the number of basis functions per atom.

As stated above, specific mathematical equations are required. For my research, the model chemistry used is B3LYP and will have three different basis sets. The first basis set used is 3-21G, which will provide a more accurate representation of orbitals. The second basis set being used is 6-31G(*d*). This basis set adds polarization functions to heavier atoms. Instead of using the three-component type function it will be using the six-component type *d* function. Lastly, 6-31+G(*d,p*) will be used. It adds *p* functions to hydrogens as well as still using polarization functions from the previous basis set. The Gaussian program uses the Schrodinger equation:

$$i\hbar \frac{\partial}{\partial t} \Psi(\mathbf{r}, t) = \hat{H} \Psi(\mathbf{r}, t)$$

To calculate the energy for the Cu(I)-S model used, (*i*) is the imaginary unit,  $\Psi(\mathbf{r}, t)$ , is the wave function, which is the probability amplitude for the different configurations of the system, and  $\hat{H}$  is the Hamiltonian operator. This program allows the user to select different ways to find the energy levels. The lowest energy found is the best and most stable structure.<sup>18,19</sup>

There are three steps to each test run. Each step will require a specific amount of time based on the basis set used with the model B3LYP. For step one a specific input command is needed to help set up the program properly. After the command B3LYP/3-21G is put in, right next to it the command (stable = opt) is required. Then Gaussian is left to run. Once the test finishes the second command step is changing the command (stable = opt) to (guess = read scf(maxcycle = 1000)). Once again let the test run and once it is complete, the third run can be set up. The last run will require the command (opt = (noeigen, z-matrix, maxcycle = 1000) scf = (maxcycle = 1000) geom = check freq) which will replace the following command (guess = read scf(maxcycle = 1000)). The program saves its progress via checkpoint files, so when one restarts the run it can continue where it left off.

The other test runs are very similar to the first one except for the minor detail of changing the basis set to 6-31G(*d*) and 6-31 + G(*d,p*). The commands following will be the same as (stable = opt), (guess = read scf(maxcycle = 1000)), (opt = (noeigen, z-matrix, maxcycle = 1000) scf = (maxcycle = 1000) geom = check freq).

## **Data and Results**

All the bond lengths were carefully checked once deleting atoms from the MERZOY image and reconstructed for the Cu-S bonds. The first run went well with the model B3LYP/3-21G (Table 1). The model system obviously changed via bond lengths yet there were no significant numbers that would assume a problem with the test run. Thus using the basis set 3-21G was successful. The second test run using the basis set 6-31G(*d*) did not turn out as expected. From the results shown in Table 1, Sulfurs 2 and 8 are significantly longer than Sulfurs 3 and 11. From Figure 1 it is clear that the test was

not successful. Sulfurs 2 and 8 have reached farther than expected from Copper that they bound themselves to Sulfurs 3 and 11. The same can be said in the third test run that the bond distances of Sulfurs 3 and 11 are much longer than those of the standard and from 3-21G.

Table 1

*Computed Angles of the First Run*

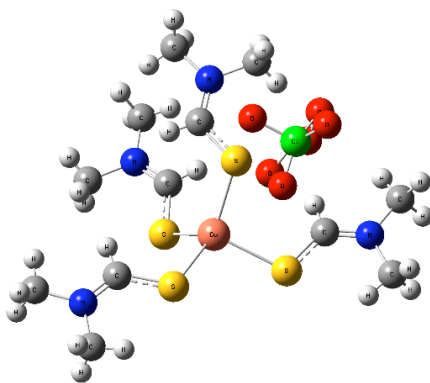
	<b>Experimental Distances (Å)</b>	<b>3-21G Computed Distances (Å)</b>	<b>6-31G(d) Computed Distances (Å)</b>	<b>6-31+G(d,p) Computed Distances (Å)</b>
Cu to 2S	2.32	2.15	3.17	2.22
Cu to 8S	2.32	2.43	3.16	2.22
Cu to 3S	2.30	2.43	2.13	3.30
Cu to 11S	2.30	2.15	2.13	3.31
2S to 4C	1.66	1.89	1.83	1.84
4C to 5H	1.07	1.09	1.09	1.08
4C to 16H	1.07	1.09	1.09	1.09
4C to 17H	1.07	1.09	1.09	1.09
8S to 9C	1.66	1.90	1.83	1.84
9C to 10H	1.07	1.08	1.09	1.08
9C to 14H	1.07	1.08	1.09	1.09
9C to 15H	1.07	1.09	1.09	1.09
3S to 5C	1.66	1.90	1.83	1.83
5C to 7H	1.07	1.08	1.09	1.09
5C to 20H	1.07	1.09	1.09	1.09
5C to 21H	1.07	1.08	1.09	1.09
11S to 12C	1.66	1.89	1.83	1.83
12C to 13H	1.07	1.08	1.09	1.09
12C to 18H	1.07	1.09	1.09	1.09
12C to 19H	1.07	1.08	1.09	1.09

Table 2 represents the computed angles from the three runs. The first run (B3LYP/3-21G) had much better results than the second (B3LYP/6-31G(*d*)) and third (B3LYP/6-31+G(*d,p*)) because of how the molecule stabilized itself. Some of the resulting angles from the second to third run raise the question of which really is the more stable molecular system. Although the results are flawed from the second and third run, the data remains valid. Further study will inquire that possibly a new model chemistry should be used because B3LYP might not be able to give the desired results when using more complex basis sets.

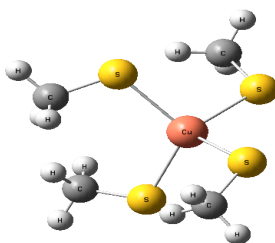
Table 2

*Computed Angles of the Three Runs*

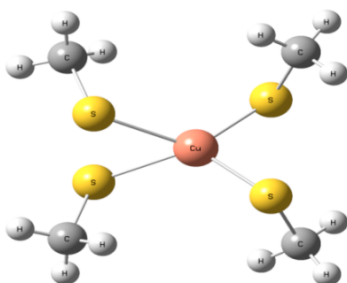
	<b>Experimental Angles</b>	<b>3-21G Computed Angles</b>	<b>6-31G(<i>d</i>) Computed Angles</b>	<b>6-31+G(<i>d,p</i>) Computed Angles</b>
11S to Cu to 2S	91.15°	86.73°	142.0°	38.83°
11S to Cu to 8S	132.3°	124.3°	41.45°	143.6°
11S to Cu to 3S	101.4°	135.2°	168.3°	107.0°
2S to Cu to 8S	113.7°	135.2°	160.2°	177.2°
2S to Cu to 3S	132.4°	124.3°	41.2°	142.6°
2S to Cu to 11S	91.15°	86.73°	142.0°	38.83°
8S to Cu to 3S	91.13°	57.76°	141.6°	38.95°
8S to Cu to 11S	132.3°	124.3°	41.45°	143.6°
8S to Cu to 2S	113.7°	135.2°	160.2°	177.2°
3S to Cu to 11S	101.4°	135.2°	168.3°	107.0°
3S to Cu to 2S	132.4°	124.3°	41.19°	142.6°
3S to Cu to 8S	91.13°	57.76°	141.6°	38.95°



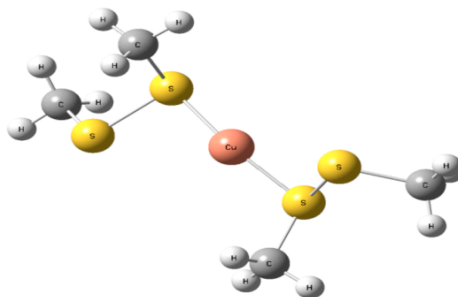
*Figure 3.* Merzoy molecule. The experimental model was used in all computed values obtained for the Cu(I) tetrahedral system. Figure generated in GaussView03 and crystal structure obtained from Cambridge Crystallography Databank.



*Figure 4.* Cu-cysteinyl sulfur model. The model was taken from the MERZOY crystal structure above and used as the starting for all calculations within the study.



*Figure 5.* Cu-cysteinyl molecule after B3LYP/3-21g calculations.



*Figure 6.* Cu-cysteinyl molecule after B3LYP/6-31g (d) calculations.

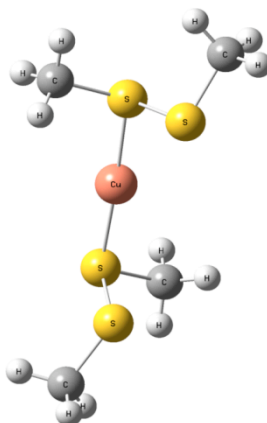


Figure 7. Cu-cysteinylyl molecule after B3LYP/6-31+g (d,p) calculations.

## Discussion

The results given from Table 1 shown above clearly show some good representations. It appears that the Sulfur-Carbon bonds and Carbon-Hydrogen bonds did not vary as much from the experimental model. What tended to vary the most had been the Copper-Sulfur bonds especially from the level of theories of B3LYP/6-31G and B3LYP/6-31+G(*d,p*).

B3LYP/3-21G provided good results as compared to the starting experimental model. The final overall results will not be based off this level of theory because using the basis set 3-21G will not show the lowest energies, a more complex basis set will need to be used because 3-21G is one of the simplest basis sets. B3LYP/6-21G(*d*) and B3LYP/6-31+G(*d,p*) did not provide good results as compared to the starting experimental model. The overall problem which occurred is still unknown, but it would seem that possibly the model chemistry needs to be modified.

## **Conclusion and Future Direction**

We now need to go back to the original model used and re-evaluate the bond lengths and angles. We will use different model chemistry, which is M052X, but with the same basis sets. At this time a new run is being processed with the basic basis set of 3-21G to evaluate at least some similarities to using the level of theory B3LYP/3-21G. If similar results occur, then more advanced basis sets will be used to calculate the energies and hopefully the structural systems will come to a more appealing system. One other possibility could have been the basis sets chosen might have not been very compatible with this model chemistry; thus, it did not represent the final structural system. Further experiments are planned to investigate this matter in the future.

## **Acknowledgments**

I, Robert E. De Vasto of the 2009 class of Cabrini College, would like to acknowledge my mentor, Dr. Melinda Harrison, for her complete guidance and support with accepting myself as an advisee for this research project. I has been a great experience that could not have occurred if not for all of Dr. Melinda Harrison's help. I would also like to thank Dr. Jeff Evanseck of Duquesne University in guiding me further into computational chemistry while advancing my knowledge on the research by Dr. Melinda Harrison.

I give my gratitude to Cabrini College and Duquesne University for the availability of their resources and a great opportunity.



## References

1. Harrison, M. D., et al. (2000). Intracellular copper routing: The role of copper chaperones. *Trends in Biological Sciences*, 25, 29–32.
2. Harrison, M. D., Jones, C. E., & Dameron, C. T. (1999). Copper chaperones: function, structure and copper-binding properties. *Journal of Biological Inorganic Chemistry*, 4, 145–153.
3. Dameron, C. T., & Harrison, M. D. (1998). Mechanisms for protection against copper toxicity. *American Journal of Clinical Nutrition*, 67, 1091S–1097S.
4. Arnesano, F., et al. (2001). Characterization of the binding interface between the copper chaperone Atx1 and the first cytosolic domain of Ccc2 ATPase. *Journal of Biological Chemistry*, 276(44), 41365–41376.
5. Zhiguang X., Graham, F. L., George, N., Howlett, G. J., & Wedd, A. G. (2004). C-terminal domain of the membrane copper transporter Ctrl from *Saccharomyces cerevisiae* binds four Cu(I) ions as a cuprous-thiolate polynuclear cluster: Sub-femtomolar Cu(I) affinity of three proteins involved in copper trafficking. *Journal of the American Chemical Society*, 126, 3081–3090.
6. Brown, K., et al. (2002). Structures of the cuprous-thiolate clusters of the Mac1 and Ace1 transcriptional activators. *Biochemistry*, 41(20), 6469–6476.
7. Ioanna Anastassopoulou, L. B., Bertini, I., Cantini, F., Katsari, E., & Rosato, A. (2004). Solution structure of the Apo and copper(I)-loaded human metallochaperone HAH1. *Biochemistry*, 43, 13046–13053.
8. Carnie Abajian, L. A. Y., Ramirez, B. E., & Rosenzweig, A. C. (2004). Yeast Cox17 solution structure and copper(I) binding. *The Journal of Biological Chemistry*, 279(51), 53584–53592.
9. Banci, L., et al. (2001). Solution structure of the yeast copper transporter domain Ccc2a in the apo and Cu(I)-loaded states. *Journal of Biological Chemistry*, 276(11), 8415–8426.
10. Lucia Banci, I. B., Cantini, F., Ciofi-Baffoni, S., Gonnelli, L., & Mangani, S. (2004). Solution structure of Cox11, a novel type of B-immunoglobulin-like fold involved in Cu B site formation of cytochrome c oxidase. *The Journal of Biological Chemistry*, 279(33), 34833–34839.
11. Cobine, P. A., Jones, C. E., & Dameron, C.T. (2002). Role for zinc(II) in the copper(I) regulated protein CopY. *Journal of Inorganic Biochemistry*, 88(2), 192–196.
12. Wernimont, A. K., et al. (2000). Structural basis for copper transfer by the metallochaperone for the Menkes/Wilson disease proteins. *Nature Structural Biology*, 7(9), 766–771.

13. Dance, I. G., & Calabrese, J. C. (1976). The crystal and molecular structure of the Hexa-( $\mu_2$ -Benzenethiolato)tetracuprate(I) Dianion. *Inorganica Chimica Acta*, 19, 141–142.
14. Presta, A., Fowle, D. A., & Stillman, M. J. (1997). Structural model of rabbit liver copper metallothionein. *Journal of the American Chemical Society, Dalton Transactions: Inorganic Chemistry*, \_\_ (6), 977–984.
15. Boris Ni, J. R. K. (2003). An ab Initio and AIM study on the molecular structure and stability of small Cu (x) S (y)- clusters. *Journal of Physical Chemistry A*, 107(16), 2890–2897.
16. Carlo Mealli, S. S. M. C. G. a. M. J. C. (2001). Theoretical analysis of bonding and stereochemical trends in doubly bridged copper(I)-copper(I) dimers. *Organometallics*, 20, 1734–1742.
17. Todor Dudev, C. L. (2002). Factors governing the protonation state of cysteines in proteins: An ab initio/CDM study. *Journal of the American Chemical Society*, 124(40), 6759–6766.
18. Frisch, M. J., G. W. T., Schlegel, H. B., Scuseria, G. E., Robb, M. A., Cheeseman, J. R., Montgomery, Jr., J. A., et al. (2003). *Gaussian03*. Pittsburgh, PA.
19. Harrison, M. (2007). *Transfer of Cu(I) between metal binding sites and the development of Cu(I) forcefield parameters using CHARMM* (p. 1–149). Pittsburgh, PA: Duquesne University.

13. Dance, I. G., & Calabrese, J. C. (1976). The crystal and molecular structure of the Hexa-( $\eta^2$ -Benzenethiolato)tetracuprate(I) Dianion. *Inorganica Chimica Acta*, 19, 141–142.
14. Presta, A., Fowle, D. A., & Stillman, M. J. (1997). Structural model of rabbit liver copper metallothionein. *Journal of the American Chemical Society, Dalton Transactions: Inorganic Chemistry*, \_\_ (6), 977–984.
15. Boris Ni, J. R. K. (2003). An ab Initio and AIM study on the molecular structure and stability of small Cu (x) S (y)- clusters. *Journal of Physical Chemistry A*, 107(16), 2890–2897.
16. Carlo Mealli, S. S. M. C. G. a. M. J. C. (2001). Theoretical analysis of bonding and stereochemical trends in doubly bridged copper(I)-copper(I) dimers. *Organometallics*, 20, 1734–1742.
17. Todor Dudev, C. L. (2002). Factors governing the protonation state of cysteines in proteins: An ab initio/CDM study. *Journal of the American Chemical Society*, 124(40), 6759–6766.
18. Frisch, M. J., G. W. T., Schlegel, H. B., Scuseria, G. E., Robb, M. A., Cheeseman, J. R., Montgomery, Jr., J. A., et al. (2003). *Gaussian03*. Pittsburgh, PA.
19. Harrison, M. (2007). *Transfer of Cu(I) between metal binding sites and the development of Cu(I) forcefield parameters using CHARMM* (p. 1–149). Pittsburgh, PA: Duquesne University.